Universidad del País Vasco Euskal Herriko Unibertsitatea
BILBOKO INGENIARITZA ESKOLA
ESCUELA DE INGENIERÍA DE BILBAO

MÁSTER UNIVERSITARIO EN

INGENIERÍA INDUSTRIAL

TRABAJO FIN DE MÁSTER

BLADE PITCH MECHANISM DESIGN AND CONTROL FOR A SMALL WIND TURBINE

Estudiante *Roggero Asensio, María*
Director/Directora *Herrero Villalibre, Saioa*
Curso académico *2020-2021*

Bilbao, 14-09-2021

University of Applied Sciences

HOCHSCHULE EMDEN·LEER

Blade pitch mechanism design and control for a small wind turbine

Master thesis

Maria Roggero Asensio
Industrial engineering
Matriculation number: 7020891

08.2021

First supervisor: Prof. Dr. –Ing. Iván Herráez
Second supervisor: Mohsen Forghani

Fachbereich Technik
Maria Roggero Asensio

University of Applied Sciences
HOCHSCHULE EMDEN·LEER

E R K L Ä R U N G

[ ] Die vorliegende Arbeit enthält vertrauliche / kommerziell nutzbare Informationen, deren Rechte außerhalb der Hochschule Emden/Leer liegen. Sie darf nur den am Prüfungsverfahren beteiligten Personen zugänglich gemacht werden, die hiermit auf ihre Pflicht zur Vertraulichkeit hingewiesen werden (Sperrvermerk).

[X] Soweit meine Rechte berührt sind, erkläre ich mich einverstanden, dass die vorliegende Arbeit Angehörigen der Hochschule Emden/Leer für Studium / Lehre / Forschung uneingeschränkt zugänglich gemacht werden kann.

E I D E S S T A T T L I C H E V E R S I C H E R U N G

Ich, der/die Unterzeichnende, erkläre hiermit an Eides statt, dass ich die vorliegende Arbeit selbständig verfasst habe und keine anderen als die angegebenen Quellen und Hilfsmittel benutzt habe. Alle Quellenangaben und Zitate sind richtig und vollständig wiedergegeben und in den jeweiligen Kapiteln und im Literaturverzeichnis wiedergegeben. Die vorliegende Arbeit wurde nicht in dieser oder einer ähnlichen Form ganz oder in Teilen zur Erlangung eines akademischen Abschlussgrades oder einer anderen Prüfungsleistung eingereicht.

Mir ist bekannt, dass falsche Angaben im Zusammenhang mit dieser Erklärung strafrechtlich verfolgt werden können.

_____

Ort, Datum, Unterschrift

Abbreviations

Vertical Axis Wind Turbine .....VAWT

Horizontal Axis Wind Turbine .....HAWT

Small Wind Turbine .....SWT

Small Wind Turbine Competition .....ISWTC

Hanze University of Applied Sciences .....HUAS

Symbols

E	Wind energy in mass units
m	Displaced air mass
v	Air mass velocity
e	Produced energy per volume unit
ρ	Air density
$\dot{Q}$	Volume flow rate of air
P	Air power
A	Area
D	Diameter
C_p	Power capture coefficient
P_{rotor}	Rotor power
λ	Tip speed ratio
α	Angle of attack
F_L	Lift force
F_D	Drag force
C_L	Lift coefficient
C_D	Drag coefficient
c	Cross-section chord
F_{act}	Actuator force
T_s	Aerodynamic torque
x	Mechanism displacement

x_{min}	Minimum linear position
x_{max}	Maximum linear position
R	Length in mm of the Clevis
L	Length in mm of the linkage
β	Angle between the reference line and the clevis
γ	Angle between the reference line and the linkage
J_{blade}	Rotating inertia of the blade and motor
D_{blade}	Pitch system coefficient of the viscous friction
K	Pitch system spring constant
T_s	Actuation torque applied by the servo motor on the blade shaft
T_R	External resistance torque applied in the blade,
J_{blade}	Rotating inertia of the blade and motor
D_{blade}	Pitch system coefficient of damping
K	Pitch system stiffness coefficient
V_R	Relative velocity

Key Word

Pitch mechanism, pitch control, airfoils, lift force, aerodynamic loads, rotor, blade, power coefficient, Arduino, Cad modelling, small wind turbines.

Table of Contents

1. Preface 1
2. Introduction 2
2.1. Types of wind turbines (Classification) 2
2.1.1. According to the orientation of the axis of rotation 2
2.1.2. According to wind orientation 3
2.1.3. According to the number of blades 4
2.2. Horizontal axis wind turbine (HAWT) components 6
2.3. Aerodynamics and its application in wind turbines 7
2.3.1. Theory of quantity of movement 8
2.3.2. Power capture coefficient (Cp) and Betz limit 9
2.3.3. Blade profile aerodynamics characteristics 11
2.4. Wind turbine control strategy 13
2.4.1. Pitch control 14
2.4.2. Passive stall control 15
2.4.3. Active stall control 15
3. International small wind turbine contest 16
3.1. Design requirements 16
3.2. Wind turbine of the University of Applied Science Emden 17
3.2.1. Design description 17
4. Design of the pitch mechanism 24
4.1. Preliminary design calculations 24
4.2. Equations of motion for blade pitch system 29
4.3. Actuator selection 35
4.4. Pitch Mechanism CAD design 37
4.5. Manufacturing and construction of the pitch mechanism 42
5. Control system 46
5.1. Closed-loop control system types 47
5.1.1. ON/OFF control system 47
5.1.2. PID control system 48
5.2. Control system components 52

5.2.1. Actuator 53
5.2.2. Arduino Nano 54
5.2.3. Channel Relay module 55
5.2.4. Push button 56
5.2.5. Potentiometer 58
5.3. Software implementation 60
5.3.1. Pitch mechanism position control 60
5.4. Control implementation and testing 64
6. Planning and budget 72
6.1. Planning 72
6.2. Budget 75
7. Conclusion 76
8. References 77

List of Figures

Figure 1: Horizontal Axis Wind Turbine (HAWT) [3] 2
Figure 2: Vertical Axis Wind Turbine (VAWT) [4] 3
Figure 3: Upwind (a) and downwind (b) wind turbines. [6] 3
Figure 4: Designs of HAWTs: a) three-bladed, b) two-bladed, c) single-bladed, d) multibladed, e) multi-bladed with diffuser [7] 4
Figure 5: Performance coefficient of various designs of wind turbine rotors. [9] 5
Figure 6 Most relevant components of a HAWT [2] 6
Figure 7 Wind energy extraction [11] 8
Figure 8: Comparison of wind power, usable energy (Betz-limit) and power output [14] 10
Figure 9 Power coefficient curves as a function of tip speed ratio and pitch angles [15]. 10
Figure 10 Rotor of a three-bladed wind turbine with rotor radius R [16] 11
Figure 11: Blade profile of an HAWT [10] 12
Figure 12: Drag and Lift forces [17] 12
Figure 13: Power-speed curves for Pitch, Stall and Active Stall Control [18] 14
Figure 14: Power curves of fixed pitch and variable pitch wind turbines. [20] 14
Figure 15 Hochschule Emden´s designed wind turbine 17
Figure 16 Airfoil E216 18
Figure 17 Reference system on blades 18
Figure 18 Blade connection to the mounting pin 19
Figure 19 Hub design front and back sides 19
Figure 20 Blades and hub overview 20
Figure 21 Nacelle components overview 20
Figure 22 Connection of cable to actuator 21
Figure 23 Section view of the powertrain 21
Figure 24 Generator Arend D80 PMG 22
Figure 25 Nacelle cover 22
Figure 26 Manufactured tower of the wind turbine 23
Figure 27 Available space in the shaft 24
Figure 28 A Slide-crank mechanism scheme 25
Figure 29 Dead point position of the mechanism 25
Figure 30 Representation of the mechanism in the remarkable positions 26
Figure 31 Pitch mechanism at the maximum linear position 26
Figure 32 Right triangles used to obtain the relation of the pitch angle and linear movement 27
Figure 33 Pitch angle range in as a function of the variables R and L (Eq.17) 28
Figure 34 Relation between beta and the possible values of R and L to be considered 29
Figure 35 Representation of the blade rotating mass model 29
Figure 36 Relationship between actuator force and torque exerted on the blade 30
Figure 37 Relationship between the actuator force and the parameters R and L (Eq. 24) 31
Figure 38 Analysis of the mechanism in terms of linear motion 33
Figure 39 Design values for the chosen configuration (case 3) 33
Figure 40 R-L mechanism connection to the blade mountain pin 34
Figure 41 Relation between the pitch angle and beta 35

Figure 42 Chosen linear actuator model (Actuonix PQ12) 36
Figure 43 Pitch mechanism overview 37
Figure 44 Parts that conform the final pitch mechanism 37
Figure 45 Pitch disk drawing 38
Figure 46 Pitch-hub connections 38
Figure 47 Pitch mechanism front and half section view 39
Figure 48 Pitch holding drawing 39
Figure 49 Actuator and pitch mechanism connecting pieces 40
Figure 50 Crank- Slide (R-L) mechanism 40
Figure 51 Connections between the pitch mechanism and the blade pin 41
Figure 52 Overview of the pitch mechanism in the Wind Turbine 41
Figure 53 Prusa 3D printers available in the FabLab 42
Figure 54 Design of the pitch mechanism prototype 43
Figure 55 Pitch mechanism prototype overview in the wind turbine 44
Figure 56 Front and back side of the manufactured mechanism. 44
Figure 57 Prototype mechanism mounted on the shaft. 45
Figure 58 Open-loop control system diagram 46
Figure 59 Closed-loop control system diagram 47
Figure 60: ON/OFF control system performance over time. [25] 48
Figure 61: Diagram of the elements of a PID-type controller [26] 49
Figure 62: Example of a performance of a proportional control system as a function of the value of the proportional constant Kp over time. [27] 50
Figure 63: Example of the performance of an integral control system as a function of the value of Ki over time. [27] 51
Figure 64: Example of the performance of a derivative control system as a function of Kd over time. [27] 52
Figure 65 Scheme of the system elements according to their function 53
Figure 66 Actuonix PQ12 Pins 53
Figure 67 Actuator wiring connections 54
Figure 68 Arduino Nano 54
Figure 69 Arduino Nano pins connections 55
Figure 70 Relay module schematic 56
Figure 71 Relays module wiring connections 56
Figure 72 Push button wiring connections 57
Figure 73 Pull-up and pull-down resistors [29] 57
Figure 74 Potentiometer wiring connections 58
Figure 75 Potentiometer input-analog signal relation 59
Figure 76 Relationship between the potentiometer input and the pitch angle 59
Figure 77 Pitch mechanism position control diagram 60
Figure 78 Arduino code part 1: Variable declaration. 61
Figure 79 Arduino code part 2: Single Run Setup 61
Figure 80 Decision-making block diagram 62
Figure 81 Arduino code part 3: main program (Loop) 63
Figure 82 Arduino code part 4: function definitions 63

Figure 83 Temporary control circuit connections 64
Figure 84 Test 1: Potentiometers lecture....65
Figure 85 Test 2: button operation and actuator reaction 66
Figure 86 Test 3: Actuator response accuracy....66
Figure 87 Push button replacement code....67
Figure 88 Final control configuration circuit connections without push button 68
Figure 89 Actuator reaction without push button....68
Figure 90 Actuator response in a reduced interval of 1500ms 69
Figure 91 Comparation of the real and theorical pitch angle values....70
Figure 92 Normalized values of the external potentiometer and pitch angle....71
Figure 93 Work Breakdown Structure of the project 72
Figure 94 Project Gantt chart (I) 73
Figure 95 Project Gantt chart (II) 74

List of Table

Table 1 Forces and moments on the blades 19
Table 2 Values of beta for the different possible configurations of the mechanism 32
Table 3 Final configuration's most relevant parameters 34
Table 4 Specifications of the actuator (Actuonix PQ12) 36
Table 5 Pitch mechanism part list 42
Table 6 Material properties PLA 44
Table 7 Main characteristics of Arduino Nano 55
Table 8 Control elements location 60
Table 9 Cost of the components of the mechanical system 75
Table 10 Cost of the components of the control system 75

1. Preface

This master's thesis involves the design and control of the blade´s pitch angle for a small wind turbine presented to the International Small Wind Turbine Competition (ISWTC).

The control of pitch mechanism will modify the position of the wind turbine blade by means of a rotation with respect to its longitudinal axis. As a result, a better control of the wind turbine power, a reduction of aerodynamic stresses, thus facilitating better operation and maintenance will be achieved.

The main objectives of this project are as follows:

- Design the pitch mechanism
- Modelling of pitch mechanism for the controller design
- Study and understanding pitch control objectives and strategies
- Designing the controller and validating by numerical simulations
- Realization of the controller using Arduino or equivalent device

This work will start by introducing the main types of wind turbines and factors that can affect a horizontal axis generator. In addition, the aerodynamic principles that govern the operation of wind turbines are described in order to understand the importance of the pitch system. As well as a description of the blade profiles and the theories and concepts used for the aerodynamic calculations.

Once the theoretical concepts of the wind turbine have been introduce, the background of the project is presented, which includes a brief description of the wind turbine that will be used as the starting point for this project. Furthermore, the requirements specified by the competition rules are also listed.

Afterwards, the needed calculations for the design of the pitch mechanism, the selection of the actuator and the CAD design of the mechanism, as well as the actual constructed mechanism are presented. And immediately afterwards, the control systems are developed theoretically and the designs of the developed control system are described, along with the elements used and the Arduino code and the result obtained.

Lastly, the plan and budget executed for the realisation of the project as well as the conclusions are presented with some suggestions for system improvements to be considered in the future.

2. Introduction

Wind turbines are designed to capture wind energy and convert it into electrical energy [1]. The following sections will describe the principle of operation of a wind turbine and its classification as well as a summary of its components.

2.1. Types of wind turbines (Classification)

2.1.1. According to the orientation of the axis of rotation

The first and most classic classification is based on the position of its main axis, which is divided into two types: horizontal axis and vertical axis [2].

Horizontal axis wind turbines (HAWT) are so-called because their main shafts are located parallel to the ground. The connection elements, drive train, and generator are located at the height of the rotor in the nacelle located at the top of the tower, as can be seen in Figure 1. In this type of wind turbine, a higher energy production is obtained, but it is necessary to control its orientation to the wind direction.

Figure 1: Horizontal Axis Wind Turbine (HAWT) [3]

On the other hand, vertical axis wind turbines (VAWT) have the main axes perpendicular to the ground. One advantage of the use of this type of wind turbines is that they capture the wind in any direction and therefore, there is no need for orientation control. Another advantage is that the link with the drive train and generators is made on the ground and thus has a lower cost and greater simplicity when it comes to its assembly. The reason why these types of wind turbines are less used for energy production is because they have a significantly lower efficiency than horizontal axis wind turbines.

Figure 2: Vertical Axis Wind Turbine (VAWT) [4]

2.1.2. According to wind orientation

This classification only makes sense for HAWTs because the VAWTs do not need a wind orientation system, as we have already mentioned. Therefore, the HAWTs can be classified into two different types according to the wind orientation [2]:

- Upwind: The air encounters the rotor before the tower. They are more efficient than downwind wind turbines as they do not present an aerodynamic interference with the tower. However, they have the disadvantage of not automatically aligned with the wind direction, so they need to have an orientation element in the nacelle [5].
- Downwind: The air encounters the tower before the rotor. A yaw system is not necessary as they are automatically aligned with the wind direction, but they are less efficient than upwind wind turbines [5]. The automatic orientation of the downwind turbine occurs because the blades have a certain taper with respect to the axis of rotation. When the wind direction changes, due to the conicity of the blades, a momentum is created that rotates the whole assembly (rotor, nacelle and hub) to align with it.

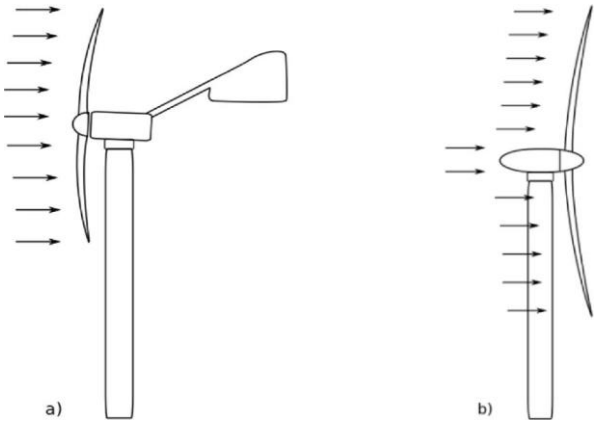

Figure 3: Upwind (a) and downwind (b) wind turbines. [6]

2.1.3. According to the number of blades

Within the HAWTs classification we can find another one, which depends on the number of blades that th wind turbine has. Four types of wind turbines can be distinguished: single-bladed, two-bladed, three-bladed, and multi-bladed. Below the different types are described.

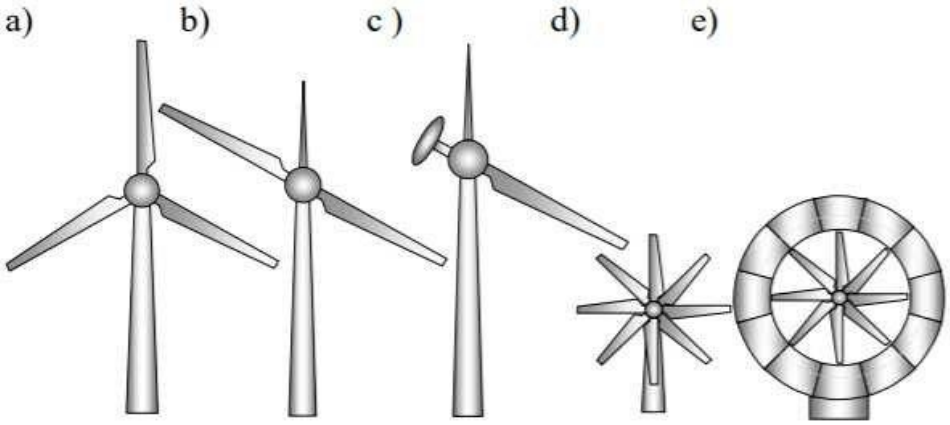

Figure 4: Designs of HAWTs: a) three-bladed, b) two-bladed, c) single-bladed, d) multibladed, e) multi-bladed with diffuser [7]

2.1.3.1. Three-bladed

This is the most widespread design in the wind production market as it is the one that offers the best performance. The rotor consists of 3 blades forming 120° between each one of them. Owing to the characteristics of their moment of inertia, they have the advantage of a smoother and more uniform rotation.

This fact minimizes the stresses on the blades or the structure. It is the rotor design that requires the least speed to produce the same electrical power. As the rotational speed of the wind turbine is lower, noise generation is reduced. In addition, the track life of the components is extended and maintenance costs are reduced.

2.1.3.2. Two-bladed

Two bladed wind turbines reduce the cost of mass and, therefore, of material with respect to the three-bladed one. However, it has the disadvantage of suffering greater dynamic stresses. As it has an even number of blades, as soon as one of them passes through the tower, it stops receiving wind, in other words, result what is known as tower shadow. This causes an instability of moments in the rotor that leads to the appearance of great stresses at the base of the opposite blade, which can lead to its breakage.

Furthermore, two-bladed generators must reach a higher rotational speed than three-bladed generators to produce the same electrical power. A higher speed means more pronounced wear of shafts, bearings, ..., and also leads to an increase in noise levels [8].

2.1.3.3. Single-blade

Single bladed wind turbines present a reduction in mass and cost with respect to the two-bladed rotor. However, this weight reduction is focused more on the gearbox and the generator than on saving a rotor blade. This is because a blade counterweight is necessary to avoid unstable turbine operation leading to unexpected vibrations or stresses in the structure, such as fatigue loads. Even so, manufacturing costs are reduced as there is no need to manufacture a second blade [8].

2.1.3.4. Multi-bladed

Multi-bladed wind turbines are used as small turbines, mainly for water pumping applications. They usually have between 12 and 24 blades. This configuration has a high starting torque, rotating at low speeds. They are not used for electricity generation, as in the design of wind turbines for electricity generation it is convenient for the rotor to rotate at the highest possible number of revolutions due to the reduction in size and weight of the electrical generator and the drive train, with the consequent reduction in the cost of the machine [8].

Figure 5 shows how the power coefficient (related to turbine efficiency) varies according to the tip speed ratio. This last term is the relationship of the velocity at the extreme end of the blade and the wind speed.

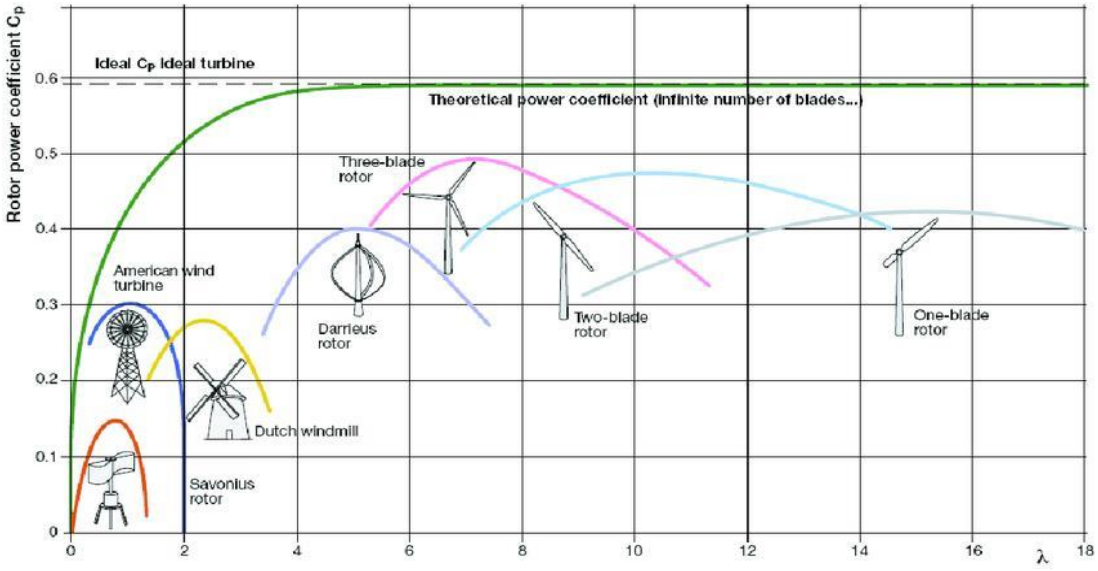

Figure 5: Performance coefficient of various designs of wind turbine rotors. [9]

As can be seen in Figure 5, HAWTs have the highest power coefficient. Within them, it can be observed that the higher the number of blades, the more efficient the generator tends to be. The

fact that there are no high-power generators with a number of blades greater than 3 is due to the following points:

- A higher number of blades means a higher initial cost of the project.
- The efficiency gained by increasing the number of blades is increasingly less significant and does not make up for the additional manufacturing and installation costs of the turbine (going from 3 to 4 blades only increases the power coefficient by around 0.5%).
- The most economically profitable option after the three-bladed rotor would be a four-bladed wind turbine. However, in this case the problem of tower shadow would arise, which would cause the instability of the structure and fatigue loads.

For these reasons, the most widespread type of wind turbine in the production of electricity from wind energy is the three-bladed wind turbine.

2.2. Horizontal axis wind turbine (HAWT) components

In this section, the most important parts of an onshore horizontal axis wind turbine will be defined and explained (Figure 6). The main components are the rotor and hub, the nacelle, and the tower and they will be described below.

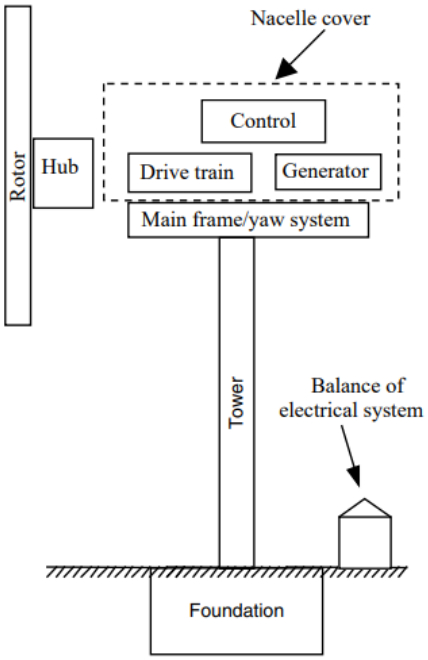

Figure 6 Most relevant components of a HAWT [2]

- The rotor blades: They capture the wind and transmit its power to the hub [10].
- Hub: this is the element that joins all the wind turbine blades together. It is mounted on the low-speed shaft, from which the torque is transmitted to the wind turbine's power transmission [10].

- Tower: The tower gives the turbine a certain height so that it collects the wind at a greater height, thus avoiding turbulence and the consequent loss of wind speed due to elements located on the ground (trees, buildings, etc.). In addition, the wiring that transports the energy produced in the generator runs through the tower [10].

Inside the nacelle can be found the following elements:

- High-speed and low-speed shafts: they are the shafts that connects the gearbox to the hub and the rotor. The high-speed shaft has a mechanical emergency disc brake which is used in case of a failure, or while the turbine maintenance process [10].
- Drive train: is the equipment that allows to the high-speed shaft to rotate 50 times faster than the low-speed shaft [10].
- Generator: also known as an asynchronous or induction generator and it transforms the mechanical energy of rotation into electrical energy. It is made up of a rotor, which is the moving part and is responsible for generating a variable magnetic field when the blades rotate, and a stator, which is the fixed part on which the induced electric current is generated [10].
- Pitch System: this is the electronics and mechanical system that is responsible for controlling the angle of attack of the blades depending on the operating conditions at any given time.
- Brakes: There are two types of brakes: mechanical brakes and electromagnetic brakes. All wind turbines have at least one mechanical brake that causes the wind turbine to stop in case of an emergency. Normally the brake is placed on the output shaft of the gearbox, which, although the rotation speed is very high, the torque to be applied with the brake at this point is lower than on the input shaft.
- Wind vane and anemometer: the wind vane is the sensor that allows the wind direction to be determined, while the anemometer allows the wind speed value to be known at the height of the nacelle.

2.3. Aerodynamics and its application in wind turbines

The objective of this section is to understand the aerodynamic principles that govern the operation of wind turbines in order to subsequently understand the importance of the pitch system. It will also describe the blade profiles and the theoretical concepts used for the aerodynamic calculations.

Aerodynamic principles are based on the behaviour of a fluid by causing motion on a body flowing through it. To obtain the power of a wind turbine, the kinetic energy of the wind is extracted and transformed into mechanical energy, which is then converted into electrical energy. It is assumed that the affected air mass remains separated from the rest of the air that does not pass through the outline of the rotor disk (see Figure 7). Since the air inside the tube is slowed down, but not compressed, the airflow cross-section must be increased to allow the airflow to pass through at a lower velocity. This kinetic energy is extracted by pressure changes that the velocity variations produce in the blade profiles [2].

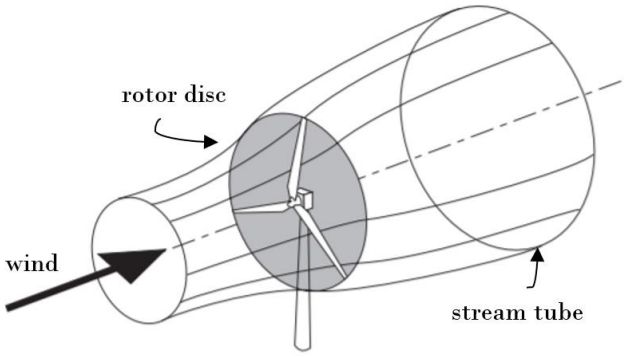

Figure 7 Wind energy extraction [11]

2.3.1. Theory of quantity of movement

As we have already mention, the wind has a certain amount of energy in its movement and this is of the kinetic energy type. If m is a mass of air moving in one direction with a velocity v, the energy that this mass has is:

$$E = \frac{1}{2} m v^2 \qquad 1$$

where,

- $E \rightarrow wind\ energy\ in\ mass\ units$
- $m \rightarrow displaced\ air\ mass$
- $v \rightarrow air\ mass\ velocity$

If we indicate it in units of volume, equation 1 takes the following form:

$$e = \frac{1}{2} \rho\, v^2 \qquad 2$$

where,

- $e \rightarrow produced\ energy\ per\ volume\ unit$
- $\rho \rightarrow air\ density$

Knowing that the volume flow rate of air $\dot{Q}$ that passes through an area A is determined by the following expression:

$$\dot{Q} = A\, v \qquad 3$$

It is possible to obtain the air power going through that certain area at a specific speed and density, and the expression of the air power is:

$$P = e\, \dot{Q} = \frac{1}{2} \rho\, A\, v^3 \qquad 4$$

The area, A, represents the circular surface that the blades cover:

$$A = \pi \frac{D^4}{4} \qquad 5$$

where,

- $D \rightarrow diameter\ of\ the\ circular\ surface\ that\ the\ blades\ cover$

From equation 4 it is possible to deduce a number of factors to be considered:

- Wind power has a strong dependence on wind speed.
- It is advisable to install wind turbines at sea level, since the greater the density of the air, the more power can be extracted from it.
- The larger the area of the blades, the more power can be extracted from the wind.

2.3.2. Power capture coefficient (Cp) and Betz limit

Even so, it is not possible to transform the entire kinetic energy of the wind into the mechanical energy used to move the rotor of the turbine. This limit does not originate from any design deficiency, but from the fact that the air arriving at the wind turbine cannot lose all its kinetic energy, as it would stop and the flow would not continue.

The optimum value that allows a constant air flow with maximum power extraction is the Betz limit. This limit establishes that any wind resource utilisation system can transform a maximum of the power indicated in equation 4. Therefore, the maximum energy that could be extracted from the air in an ideal machine would be [12]:

$$C_p = \frac{16}{27} = 59.2\% \qquad 6$$

The Betz limit provides an upper limit to the possibilities of the wind turbine, but it is not entirely realistic given that the energy transformation that takes place in a wind turbine is inevitably associated with power losses in the different components of the system.

In order to get an idea of the overall efficiency of a wind power plant, the data provided in the document "*Windenergie und ihre ausnutzung durch windmühlen*" were considered. In this document, Dr. Albert Betz formulated for the first time the theoretical maximum power that could be extracted from the wind and, in addition, the following efficiencies of the different system components were considered [13]:

- Propeller efficiency ..... 85%.
- Gearbox efficiency..... 98%
- Alternator efficiency 95%
- Transformer efficiency 98%

This results in an overall maximum efficiency of the installation of approximately 46%, Figure 8 shows the difference between the energy available from the wind, the energy set by the Betz limit, and the energy actually obtained.

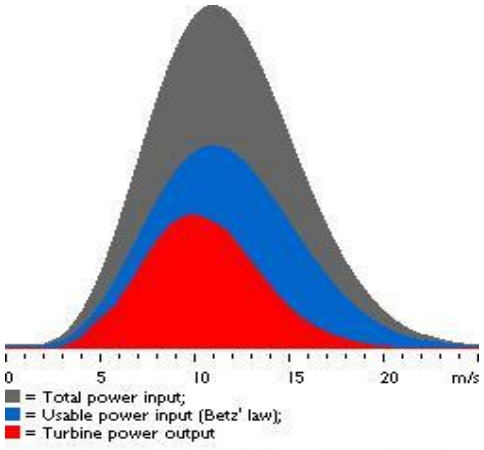

Figure 8: Comparison of wind power, usable energy (Betz-limit) and power output [14]

To represent the fraction of power extracted from the wind, it is necessary to define a new factor called the power coefficient [2]:

$$C_p = \frac{Rotor\ power}{Power\ in\ the\ wind} = \frac{P_{rotor}}{\frac{1}{2}\rho\ A\ v^3} \qquad 7$$

This power coefficient can be interpreted as the efficiency of the wind rotor and depends mainly on the wind speed, the rotational speed of the turbine and the draft angle of the blades. More concisely, this dependence can be summarised in two dimensionless parameters: the blade pitch angle, β, and the specific speed coefficient, λ, which is the ratio between the linear speed at the blade tip and the incident wind speed.

In Figure 9 it can be seen an example of the extracted power output of a horizontal axis wind turbine with a variation of the pitch angle.

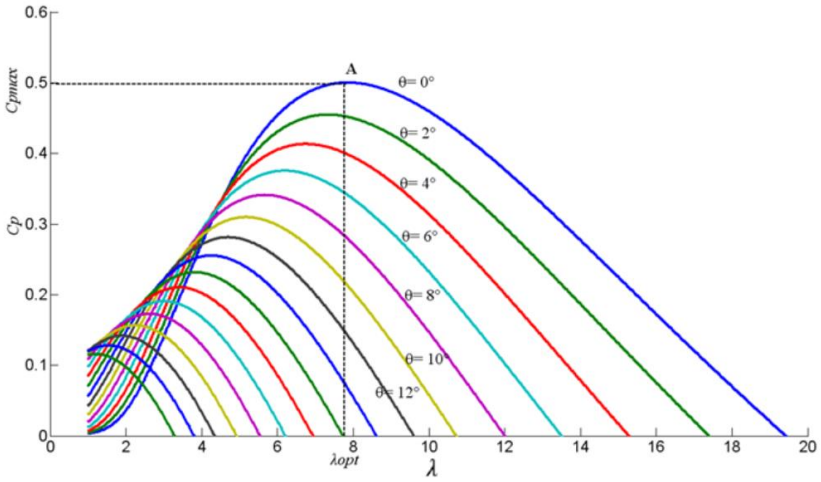

Figure 9 Power coefficient curves as a function of tip speed ratio and pitch angles [15].

Systems such as pitch control use these ratios to maintain the optimal operating point of the turbine. When the turbine starts up, for speeds lower than nominal, the wind turbine needs to get the greatest possible benefit from the wind, so the optimum value of λ is chosen for each value of the pitch angle and the one that places the wind turbine at the point of maximum power coefficient is selected (see Figure 9).

However, when the wind speed exceeds the nominal wind speed, the loads on the wind turbine could lead to a collapse, so the pitch system comes into play. The blades are now rotated about the pitch axis to let some of the air flow through and keep the generated power constant, thus lowering the power coefficient. In this way, for constant power and rotational speed, the loads on the wind turbine remain constant for rotational speeds above the rated speed.

2.3.3. Blade profile aerodynamics characteristics

For the control system design it is of great importance to know the behaviour of airfoils and the forces exerted by the wind on them.

The rotor of a wind turbine is composed of a certain number of blades. If a radial cut is made at a distance r from the axis of rotation, Figure 10, the airfoil with the angles of flow corresponding to the local element are observed, as can be seen in Figure 11.

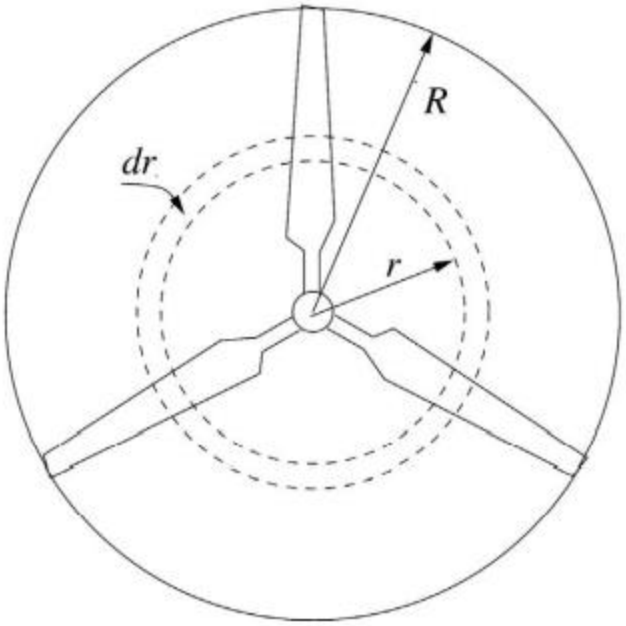

Figure 10 Rotor of a three-bladed wind turbine with rotor radius R [16]

The total local angle is the sum of the local twist angle, the angle of attack and the active or passive pitch control system angle. This twist angle is dependent on the blade geometry and invariant in time, while the pitch angle is constant along the blade but can change in time with the variation of the wind speed. For convenience, we will refer to β as the pitch angle, although it will also contain

the twist and angle of attack. As can be seen in Figure 11, the angle of attack α is the angle of attack formed by the chord line with the relative wind speed.

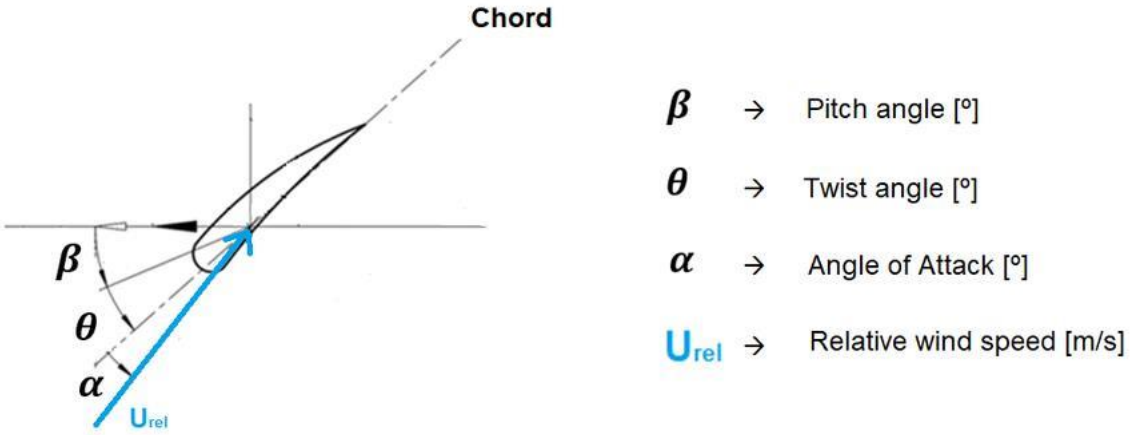

Figure 11: Blade profile of an HAWT [10]

When an airfoil is placed in a gust of air, the wind goes through the upper and lower surfaces of the blade. Due to the curvature of the blade, the air flowing on the upper side has a higher velocity than the air flowing on the lower side; according to Bernoulli's principle, the fluid particles with higher velocity will produce a low pressure on the upper side, while a higher pressure will be produced on the lower side.

This pressure difference will produce a resultant force F acting on the airfoil and it can be divided into two different forces [4] (see Figure 12):

- A component perpendicular to the incident current at infinity upstream, called lift and considered positive if it is towards the top surface.
- A component in the same direction of the undisturbed incident current, called drag.

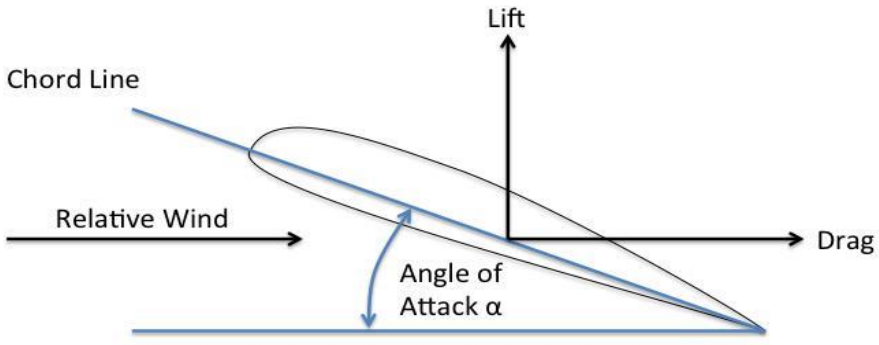

Figure 12: Drag and Lift forces [17]

The coefficients can be obtained by wind tunnel tests, measuring wind speed, lift and drag using specialised sensors. In wind turbines, the aim is to maximise lift and reduce drag. Thus, it is equally

important to place the airfoil at a suitable angle of attack so that the ratio between the drag coefficient and the lift coefficient (C_D/C_L) is reduced. It should also be mentioned that the velocity observed by the airfoil is a resultant vector called relative velocity (V_R).

The velocity of the blade section increases as a function of the radial distance from the centre of the rotor towards the blade tip, so the angle of the vector V_R varies as it approaches the base of the rotor.

In order to maintain constant, the relative velocity along the entire length of the blade and to keep the ratio (C_D/C_L) optimal throughout the blade profile, the blade is designed with a warp shape.

If the lift and drag coefficients are known, the lift and drag forces per unit length are known as well:

$$F_L = \frac{1}{2}\rho c v^2 C_l \qquad 8$$

$$F_D = \frac{1}{2}\rho c v^2 C_d \qquad 9$$

Where c is the element cross-section chord.

2.4. Wind turbine control strategy

The main objectives for power control in wind turbines should be the following:

(1) **Capture of energy from wind**: maximise energy capture considering operating constraints such as rated power, rated speed, ...
(2) **Mechanical loads**: Prevent excessive mechanical loads on the wind turbine due to sudden fluctuations in the system.
(3) **Power quality**: Condition the generated power to meet interconnection standards.

For the purposes of this thesis, the control main objective will be focused on power regulation.

For each wind turbine, the relationship between wind speed and generated power is defined by the so-called P-V curve, or power-speed curve. This curve clearly shows the cubic law between wind speed and generated power.

Most wind turbines start generating power at 2 to 3 m/s, and the rated power is reached at 12 to 13 m/s wind speed. The rated wind speed is the lowest of the wind speeds at which the wind turbine produces the rated or maximum power. Above the rated wind speed, the power cannot increase with the wind speed due to the operation of the wind turbine's power control mechanisms.

There are three ways to regulate the power output which can be seen in Figure 13 and are explained below.

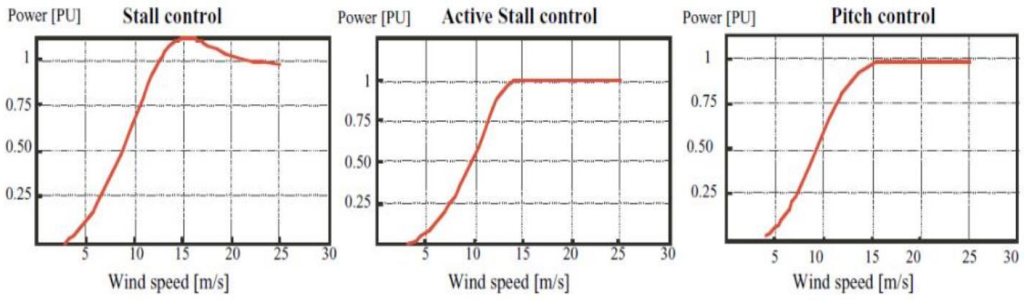

Figure 13: Power-speed curves for Pitch, Stall and Active Stall Control [18]

2.4.1. Pitch control

In blade pitch angle control systems, the rotor blades must be able to rotate around their longitudinal axis (vary the pitch angle). The reaction time of the pitch angle change mechanism is a critical factor in wind turbine design. The design of pitch-angle controlled wind turbines requires highly developed engineering to ensure that the blades rotate at exactly the desired angle [19].

This system allows a nominal power extraction for wind speeds higher than the nominal wind speed, also allowing for a safety system against high wind speeds. The disadvantages are that they require a more complicated hub design and the incorporation of mechanical, hydraulic or electronic actuators with sufficient power to move the blades.

With this type of regulation, the electronic controller checks the generated power several times per second. When this reaches a value that is too high, the controller sends a command to the pitch angle change mechanism, which immediately rotates the rotor blades slightly away from the direction of the wind flow lines. When the wind speed decreases, the blades are rotated in the reverse direction back to the position of maximum energy utilisation.

Hence, in this type of wind turbines, the computer will generally rotate the blades a few degrees each time the wind changes to maintain an optimal angle that provides maximum performance at all wind speeds [18].

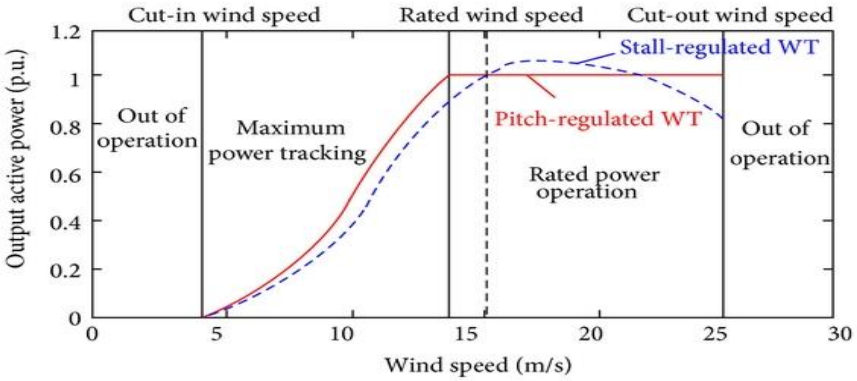

Figure 14: Power curves of fixed pitch and variable pitch wind turbines. [20]

By increasing the pitch angle when the wind increases, as the mechanical loads on the blades are reduced when the wind increases. In addition, this system dampens aerodynamic oscillations better and provides a higher starting torque than when the blade pitch is fixed. Mechanical stresses are reduced, as reducing the angle of attack also reduces lift.

2.4.2. Passive stall control

In this case the blades are attached at a fixed angle to the hub. The profile of the blade has been aerodynamically designed to ensure that turbulence is created at the back of the blade as soon as the wind speed becomes too high for the boundary layer to detach [18]. It is important to ensure that such a loss of lift does not occur abruptly, but rather gradually, for which the blade is designed slightly twisted along its longitudinal axis. The main advantage of aerodynamic stall control is that it avoids moving rotor parts and a complex control system. On the other hand, this system represents a very complex aerodynamic design problem, with the complications arising from the vibrations caused by the loss of lift [2].

In addition, there is also the inconvenient of obtaining a less regular power curve for wind values higher than nominal if compared to variable pitch regulation systems (see Figure 14). The blades, as they cannot be aligned with the wind, suffer a higher static load. These turbines also need more wind for the blades to start turning, as the starting torque is low.

2.4.3. Active stall control

In higher power wind turbines, above 1 MW, the blades can rotate only a few degrees to better adjust the stall profile. These types of machines are programmed to rotate their blades in the same way as pitch-angle control machines in order to have a reasonable high torque at low wind speeds.

However, when the machine reaches its rated power, this type of wind turbines has a major difference: if the generator is going to be overloaded, it will rotate the blades in the opposite direction to a pitch-angle control, i.e. it will increase the pitch angle of the blades to bring them to a position of higher lift loss, thus consuming the excess energy from the wind and generating turbulence [19].

The main advantage is that the output of power is more accurately controlled and the machine can operate at near rated power over a wide range of wind speeds. The control mechanism is usually hydraulic or electric as well as in the pitch control systems.

3. International small wind turbine contest

As mentioned, the pitch mechanism controller has been designed for the wind turbine submitted to the International Small Wind Turbine Contest (ISWTC). In annex A.1 and A.2 can be find the people involved in the project and the supervisors respectively.

The ISWTC is an international competition organized for the first time in 2013 by the NHL University of Applied Sciences, but it was not until 2018 when the Hanze University of Applied Sciences (Hanze UAS) organised it and since then it has been held every year in Groningen. It is a competition for the design and construction of a small wind turbine (SWT) and is open to teams of university students [21].

The contest consists of two phases, the first one is the design part, in which the team write a design report and describe the design choices, where the performance of the turbine plays an important role. The second phase is the construction part where each team realises the wind turbine proposed in the design report and as a last step tests it in the wind tunnel of the Technical University of Delft [21].

The detailed tasks that each team has to carry out and that are determined by the contest are listed below [22].

- Design a small wind turbine according to the design requirements and further conditions of the contest and write a design report on this.
- Manufacture, assemble, and test the turbine in the TU Delft wind tunnel.
- Make a product poster for display on the final symposium.
- Optional: teams are more than welcome to make a promotional leaflet for handing out during the TORQUE conference.
- Give a short 10-minute technical presentation/pitch about your design on the final symposium.

3.1. Design requirements

Due to the regulations, the contest organization has determined the design parameters [22]:

- Rotor area ≤ $2m^2$ (maximum rotor diameter $1{,}6\ m\ of\ HAWT$).
- Design height of the rotor top will not exceed 3m. Considering that the mounting pile will be provided in the contest and will also have to be considered for the final height.
- Design wind climate at hub height has to consider the following Weibull parameters: A = 5.5 m/s, k = 2.5 and standard atmospheric conditions. (Based on rural regions in Sub-Saharan Africa).
- The turbine will be provided with standard interfaces for mounting and electric connection.
- All control and safety functions must be integrated within the interface boundaries. (Remark: net power is produced at the electric interface)
- The turbine should be designed for automatic operation and achieve a maximum power output, with a DC output of 0-60 Volts and a maximum current of 20 Amps.

- The rotational speed and produced power shall under no circumstances exceed the design limits for all load cases.
- The turbine shall have provisions for a manual emergency stop and for blocking of the rotor.

3.2. Wind turbine of the University of Applied Science Emden

The following section briefly describes the components of the wind turbine designed by the Emden team.

3.2.1. Design description

The design of the wind turbine is based on the specifications of the tender (detailed in section 3.1) and from those restrictions the following parameters have been determined:

- Design point Windspeed → 7 m/s
- Maximum operating windspeed → 15 m/s
- A horizontal axis turbine with 3 Blades
- The design Betz power → $245W$
- TSR_{Design} of 4.488 (300 rpm at 7m/s)
- Power generated by the rotor at the given conditions → $117.87\ W$

Figure 15 shows an overview of the wind turbine. And afterwards, the main components will be described, which can be divided into 3 parts (as we have done in section 2.2): Rotor and hub, nacelle and tower.

Figure 15 Hochschule Emden´s designed wind turbine

- **Blades and Hub**

The basic prerequisite for an efficient wind turbine is an aerodynamically good rotor blades design. For that an airfoil Eppler 216 have been chosen (see Figure 16). Also, in order to identify possible unwanted aerodynamic behaviours of the blades before the production and to discover ways to increase efficiency, several simulations have been made by the team using CFD.

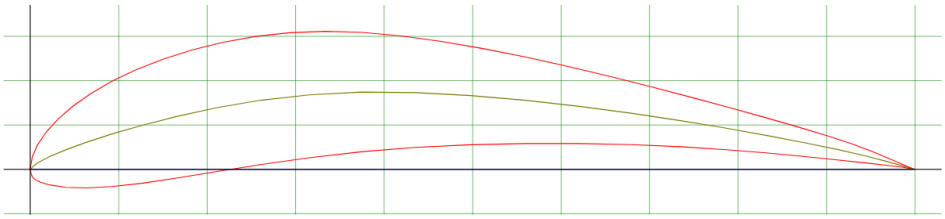

Figure 16 Airfoil E216

Once the correct design has been checked, the different forces and moments present for each of the blades have been obtained. In Figure 17 the coordinate system used to define those parameters is shown.

Figure 17 Reference system on blades

It should be pointed out that for this master thesis, given that we are going to design the mechanism that will modify the pitch angle of the blades, the mechanism has to overcome the inertia of the blades as well as the resisting torques of aerodynamic loads at the root of the blade, in this case, the y-axis resultant momentum will be considered.

Table 1 Forces and moments on the blades

	Force (N)	Momentum (Nm)
Axis x	3.22	6.43
Axis y	0.28	0.16
Axis z	12.87	-1.22

For the connection between the blade and the hub the mounting pin is used, and in order to be able to fix the blades to it several boreholes and a pocket have been made in each blade (see Figure 18).

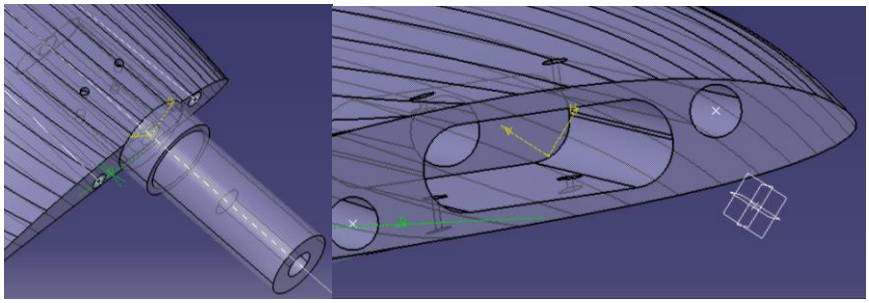

Figure 18 Blade connection to the mounting pin

Lastly, the rotor hub is the component that holds the blades and connects them to the main shaft of the wind machine. It is a key component not only because it holds the blades in their proper position for maximum aerodynamic efficiency, it transfers the rotation to the generator shaft.

For this contest the team decided that the hub will be rigidly fixed to the shaft and it have been designed from a single piece where we connect the blades, taking into consideration that the blades will have a pitching axis. Down below, in Figure 19 it can be seen a representation of the hub from the front and bac side. In order to reduce the weight of this component it has been removed some of the material without compromising the structure.

Figure 19 Hub design front and back sides

Finally, the hub and rotor assemblies are shown in the Figure 20.

Figure 20 Blades and hub overview

- **Nacelle**

The main components mounted inside the nacelle are shown in the Figure 21 and described as follows:

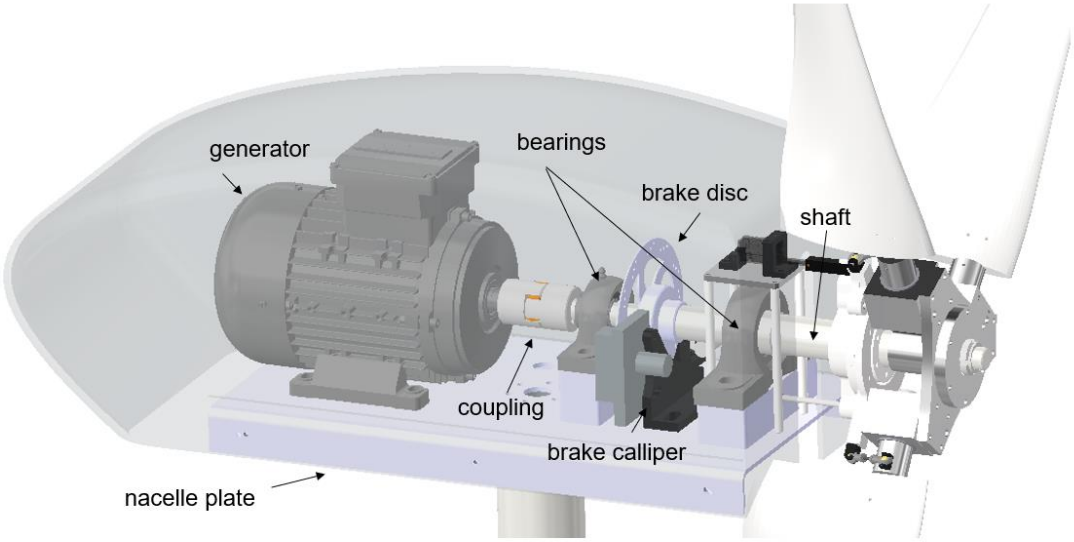

Figure 21 Nacelle components overview

- **Brake system:** The aim of our braking system is to ensure safety in the operation of the wind turbine. In order to stop the wind turbine, in case of over speeding or electrical failure, it is necessary to implement a well-suited braking system. Furthermore, the regulations demand that the system should be able to be stopped remotely from a distance of at least 10 meters [22].
  Dude to the dimensions of the actuator and the space available in the nacelle plate, the linear actuator and the brake calliper have been connected through a hole beneath the main plate (see Figure 22).

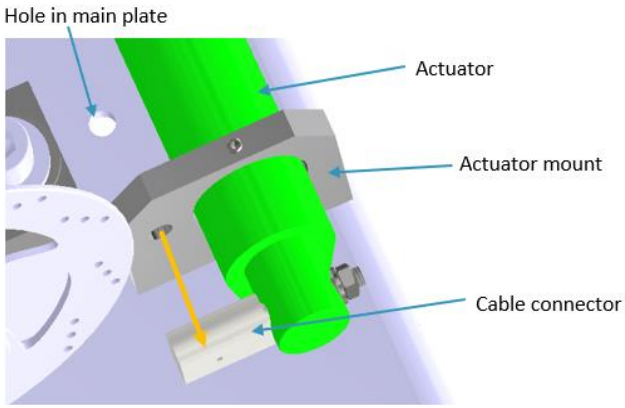

Figure 22 Connection of cable to actuator

- **Powertrain:** The powertrain transfers the power from the blades to the generator and the shaft is the central element of it. The shaft transmits the torque from the rotor to the generator and consists of many different functional sections for the individual elements mounted. These elements are shown in Figure 23.

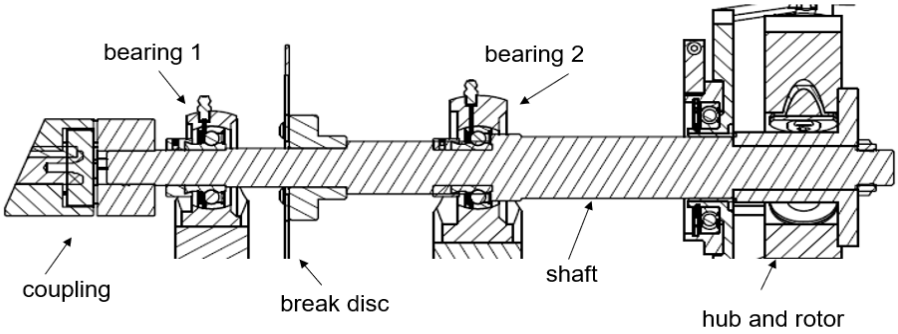

Figure 23 Section view of the powertrain

- **Bearings and couplings:** To connect the shaft with the generator different coupling and bearings have been used. As we want to have a non-switchable coupling because of the brake power which goes to the generator can be controlled, an elastic coupling has been chosen by the team.
- **Generator:** The generator will be responsible for transforming the mechanical energy coming from the shaft into electrical energy. In this case the generator that fits is the Arend D8, shown in the Figure 24.

Figure 24 Generator Arend D80 PMG

- **Nacelle cover:** The final design of the nacelle cover is shown in the Figure 25 and it has a cut-out in the front is for the shaft and the operation of the pitch mechanism actuator. There is a whole cut-out instead of hole because like this the cover can be removed pulling upwards. On each side there are three holes to assemble it with the main plate with screws.
-

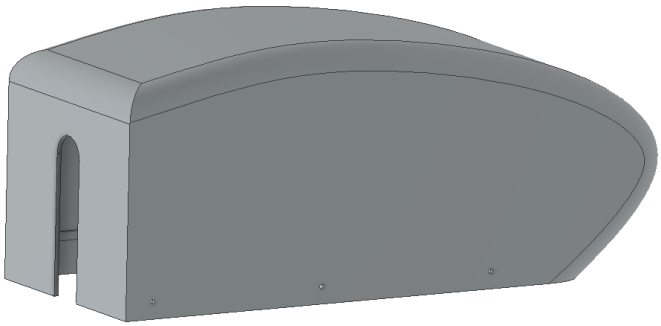

Figure 25 Nacelle cover

- **Tower**

The tower of the wind turbine holds all the elements describes above. If the tower fails and fall, it can cause extreme damage to nacelle and blades. The finite element analysis has been carried out by the team to make sure that the wind turbine stands on strong tower. However, this tower will only be used for pre-contest tests, as the tower provided by the organisers will have to be used for the final tests in the competition [22].

Figure 26 Manufactured tower of the wind turbine

- **Other components**

In order to protect the circuit boards, the battery and smaller components like voltage regulators and relays, a plastic box for electrical installation has been used, which we will refer to it as the control box in this thesis.

4. Design of the pitch mechanism

Therefore, as we have already mentioned, the pitch mechanism control will allow us, in addition to ensuring the highest slip coefficient, to regulate and control the speed of the rotor, maintaining the turbine's rotational speed between the design values even if the real wind speed is above its nominal speed.

The pitch angle is adjusted for the entire blade from its root and small variations in its value can lead to significant changes in the machine's performance. The great utility of these systems is that turbines designed to work in certain wind conditions can work optimally in other conditions by varying the pitch angle, which means that, by changing the angle we can change the characteristic curve of the wind turbine.

There are different types of mechanisms depending on the size. In larger turbines, the pitch of the blades is usually controlled by a set of gears that rotate the blades individually. But even though they are individually rotated they are usually regulated by the same controller. Thus, avoiding an uneven pitch angle as this is one of the main causes of rotor failure due to unbalanced forces on the blades.

Since our wind turbine is small and in order to use fewer components and eliminate the possibility of having unsynchronised pitching blades, it has been decided to design a pitching mechanism that launches the blades simultaneously driven by the same actuator.

The following subsections describe the design and manufacturing of the pitch mechanism.

4.1. Preliminary design calculations

The pitch mechanism will be positioned on the shaft, specifically, in the free space between the hub and the nacelle. The space available to position the mechanism and perform the control is shown in the Figure 27.

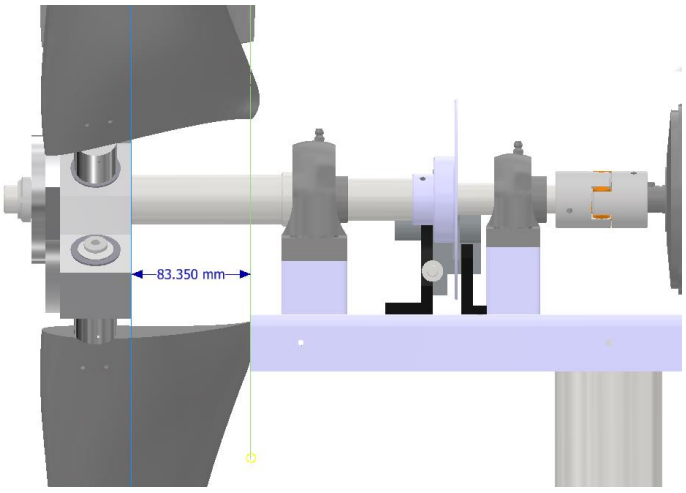

Figure 27 Available space in the shaft

Moreover, as the mechanism will be located in that space, it will limit the total course of motion of the centre of the mechanism (see Figure 28). This is why for in the following calculations it has been considered that the total displacement of the pitch mechanism will be only $20\,mm$.

Due to this limited space available, it will be necessary to carry out a kinematic and aerodynamic analysis to optimize the space as much as possible.

For the calculation, it will be considered a slide-crank type mechanism as in Figure 28, which is composed of a slider that will maintain a linear movement and the crank that will perform the rotational movement of radius (R), which will be connected by a link of length (L).

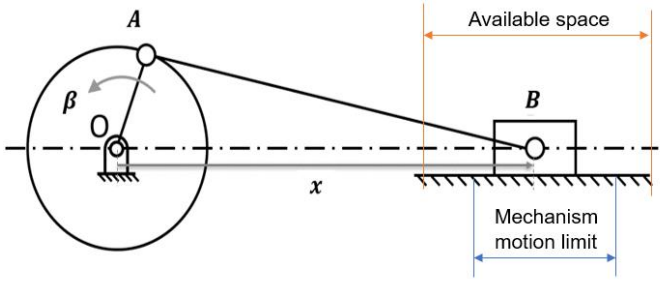

Figure 28 A Slide-crank mechanism scheme

Since the space available on the shaft is limited, it will be of vital importance to select the most suitable R and L values. Hence, there must be a compromise between the range of the pitch angle to be obtained and the force that the actuator must exert on the mechanism to obtain this angle.

First of all, the relationship between the linear movement and the pitch angle will be obtained. In order to do so, we will consider that due to the geometry of the mechanism, there will be two positions that we must avoid, known as dead points (Figure 29). As can be seen, these points take place when the linkage is linear with the connecting crank so that the mechanism tends to stop. This happens in crank-slider mechanisms when the slider is the input and the crank link is the follower.

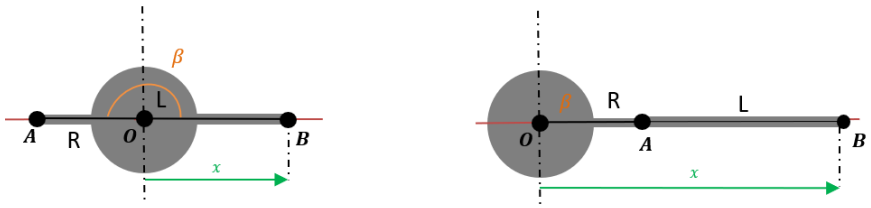

a) $\beta_{max} = 180°$ *b)* $\beta_{min} = 0°$

Figure 29 Dead point position of the mechanism

As there is a linear movement limit restriction there are two different possible configurations that can take place (see Figure 30): (a) the maximum linear position when the beta angle is minimum and b) the minimum linear position when the beta angle is maximum. Also, it can be seen in the figure the variables that will be used to calculate the limit values of the pitch angle at the available actuation range. This points are points, in which the mechanism can be locked and will need a large magnitude of external actuating force to move the mechanism from these positions.

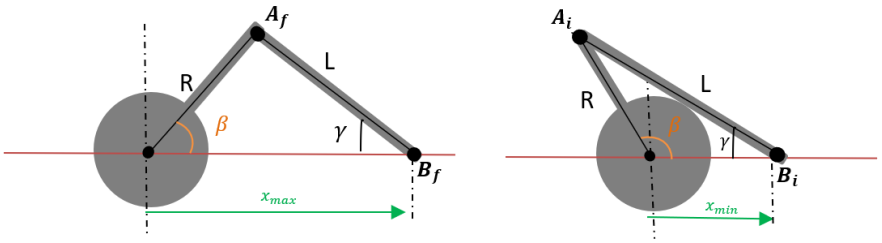

a) Maximum linear position (x_{max}) *b) Minimum linear position (x_{min})*

Figure 30 Representation of the mechanism in the remarkable positions

To perform the relation between the beta angle (β) and the actuator movement (x), it will be considered the last scenario (a), when the linear position is maximum (see Figure 31).

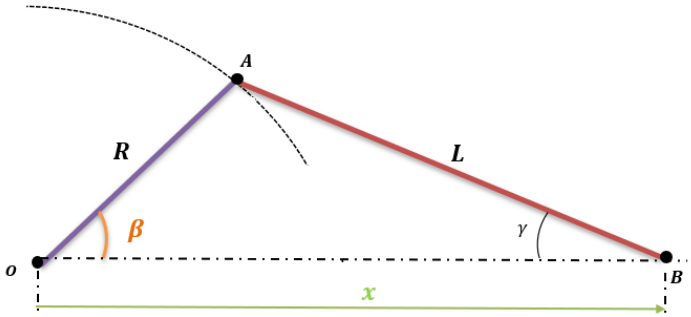

Figure 31 Pitch mechanism at the maximum linear position

Hence, we used trigonometry to obtain the equation that relates the parameters, and to make it easier, we will get two equations concerning the two right triangles that have been defined in Figure 32. As we will see, these two equations will depend on three parameters but, by combining them we will obtain the final equation needed.

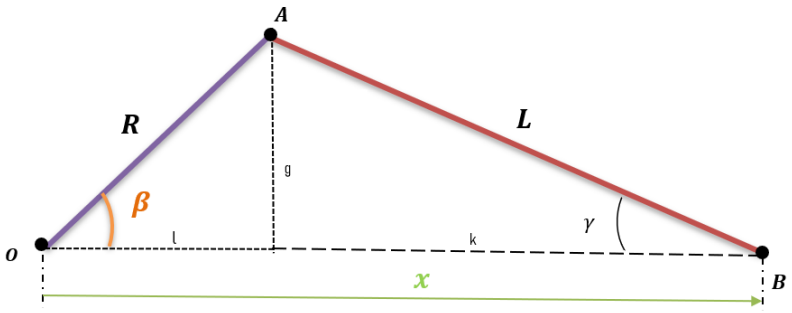

Figure 32 Right triangles used to obtain the relation of the pitch angle and linear movement

$$g = R \sin\beta = L \sin\gamma \qquad 10$$

$$x = l + k = R \cos\beta + L \cos\gamma \qquad 11$$

By clearing the term containing the angle we want to make disappear (γ) and squaring the equations, results in the following:

$$R^2 \, sin^2 \, \beta = L^2 \, sin^2 \gamma \qquad 12$$

$$x^2 + R^2 \cos^2\beta - 2xR \cos\beta = L^2 \cos^2\gamma \qquad 13$$

Adding both equations we obtain the following one:

$$x^2 + R^2(cos^2 \, \beta + sin^2 \, \beta) - 2x \, cos \, \beta = L^2 \, (sin^2 \, \gamma + cos^2 \, \gamma) \qquad 14$$

By operating to simplify equation 14 and using the following trigonometric relation (15) the angle γ will disappear and we obtain the final equation 16.

$$1 = sin^2(\beta) + cos^2(\beta) \qquad 15$$

$$x^2 + R^2 - 2x\mathrm{R} \cos\beta = L^2 \qquad 16$$

As the aim is to obtain the best values for R and L, Matlab has been used to obtain the graphs to be able to discern between those values and make a choice regarding them.

From equation 16, the relationship between the beta angle and the rest of the parameters can be obtained:

$$\beta = cos^{-1}\frac{L^2 - x^2 - R^2}{-2xR} \qquad 17$$

As we can see in Figure 33, to optimize the space available between the nacelle and the hub, it is important to use small R values. In addition, since the mounting pin of the blades has a radius of $15\ mm$, the value of R will have to be greater or equal to that value to comply with the geometry of the slider-crank mechanism. Regarding L values, to obtain a more stable movement, it is convenient to set values higher than $40\ mm$.

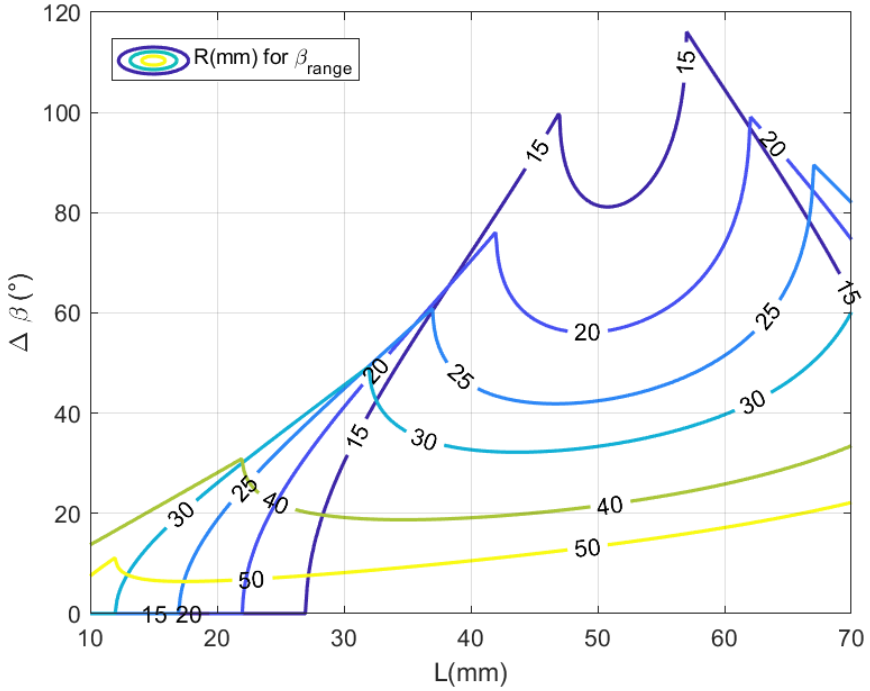

*Figure 33 Pitch angle range in as a function of the variables R and L (Eq.*17*)*

Therefore, the range of R and L values that will be taken into consideration for the comparison with the aerodynamic analysis will be 15-25 mm and 40-60 mm respectively (Figure 34).

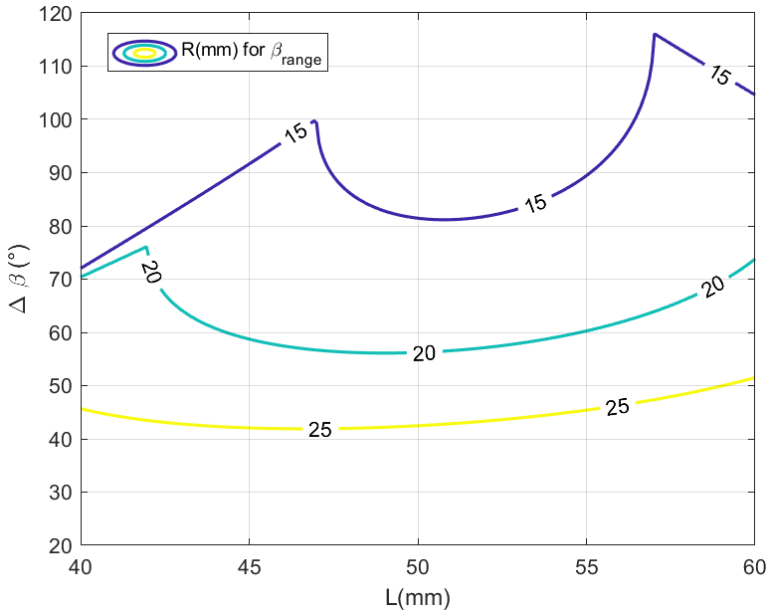

Figure 34 Relation between beta and the possible values of R and L to be considered

4.2. Equations of motion for blade pitch system

To find the necessary blade dynamic equation we will assume the rotor as a single mass system as shown in Figure 35.

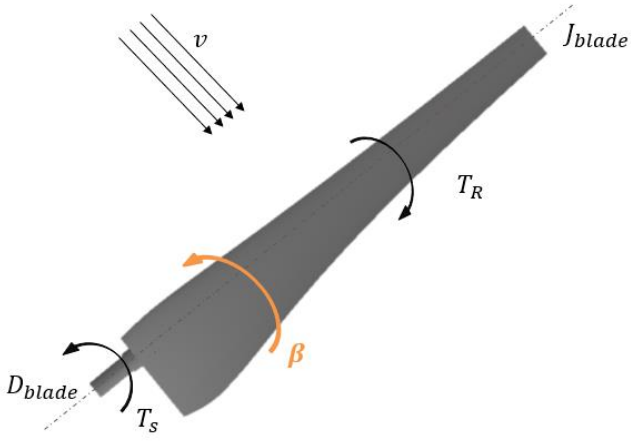

Figure 35 Representation of the blade rotating mass model

We know that the relationship between position (the pitch angle), angular speed, and angular acceleration is the following:

$$\ddot{\beta} = \frac{\partial \dot{\beta}}{\partial t} = \frac{\partial^2 \beta}{\partial t^2} \quad 18$$

Therefore, assuming the rotor as a single mass system, the dynamic equation can be developed as [2]:

$$T_s - T_R = J_{blade}\,\ddot{\beta} + D_{blade}\,\dot{\beta} + K\,\beta \quad 19$$

Where,

- $T_s \rightarrow$ Actuation torque applied by the servo motor on the blade shaft
- $T_R \rightarrow$ External resistance torque applied in the blade, caused by aerodynamic loads
- $J_{blade} \rightarrow$ Rotating inertia of the blade and motor
- $D_{blade} \rightarrow$ Pitch system coefficient of damping
- $K \rightarrow$ Pitch system stiffness coefficient

At this point two scenarios can be differentiated: when the wind turbine is in the maximum load and when the wind turbine is in the minimum load. In this last scenario the external resistance torque will be zero so the equation above will result:

$$T_s = J_{blade}\,\ddot{\beta} + D_{blade}\,\dot{\beta} + K\,\beta \quad 20$$

As far as the external force applied by the servo motor in the blade is concerned, it will be necessary to find the equation relating the actuator force and the final force exerted. This depends directly on the geometry of the pitch mechanism, i.e. the values of L and R (see Figure 36). Once again, to obtain the expression relating to these variables, the mechanism has been considered at the position of maximum linear distance (x_{max}).

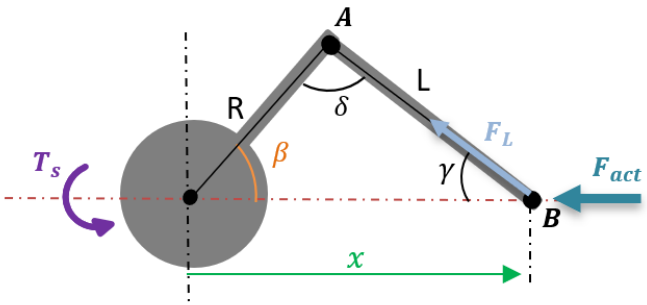

Figure 36 Relationship between actuator force and torque exerted on the blade

Analysing the forces exerted on each element of the Figure 36, we obtain the following relationships:

$$F_{act} = F_L \cos\gamma \quad 21$$

$$T_S = R\,F_L \cos(\delta - 90) = R\,T_L\ \sin\delta \quad 22$$

Replacing equation 21 in equation 22:

$$T_S = R\frac{F_{act}}{\cos\gamma}\sin\delta \qquad 23$$

Setting the equation in terms of the desired values and considering the obtained relation (Eq. 11) and the sine theorem for any triangle, the following expression is obtained:

$$\frac{Fact}{Ts} = \frac{\cos\gamma}{R\sin\delta} = \frac{\frac{x - R\cos\beta}{L}}{\frac{x}{L}R\sin\beta} = \frac{x - R\cos\beta}{x\,R\sin\beta} \qquad 24$$

Finally, Matlab has been used to obtain the graph that relates the coefficient between the force exerted by the servo and the torque that will be exerted on the blade with the different values of R and L that have been selected previously. As can be seen in Figure 37, using this relationship we manage to further reduce the values of L to between 50 and 60 mm, given that with values of less than 50 mm the curves tend to infinity and therefore, are unstable areas to be avoided.

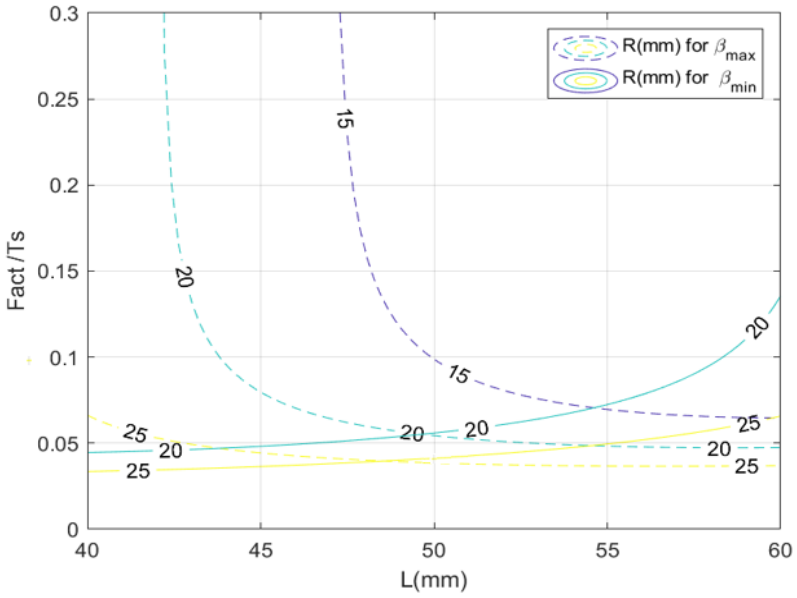

Figure 37 Relationship between the actuator force and the parameters R and L (Eq. 24)

Taking all the above into consideration, the values of beta have been calculated for the different possible configurations of the mechanism (see Table 2). From this table, four configurations have been selected according to the range of beta and will be analysed along the linear movement x. We are interested in a mechanism that makes maximum use of the available space, but it is also

of great importance that the variation of the force to be exerted by the actuator along x is as constant as possible.

Table 2 Values of beta for the different possible configurations of the mechanism

R(mm)	L (mm)	Beta min (°)	Beta max (°)	Range Beta (°)	Fact/Ts max	Fact/Ts min
15	50	32.483	113.93	81.443	0.0988	0.083498
15	52	42.788	124.57	81.785	0.080717	0.097374
15	54	51.692	137.37	85.676	0.072218	0.12429
15	56	59.893	155.55	95.656	0.067711	0.21343
15	58	67.726	180	112.27	0.065436	7.3879e+14
15	60	75.395	180	104.6	0.06469	7.3879e+14
20	50	45.314	101.54	56.223	0.054373	0.055891
20	52	51.613	108.75	57.136	0.051011	0.060884
20	54	57.623	116.59	58.968	0.048977	0.067833
20	56	63.463	125.35	61.887	0.047833	0.078192
20	58	69.216	135.58	66.368	0.047359	0.095744
20	60	74.949	148.73	73.784	0.047439	0.13555
25	50	50.568	93.03	42.462	0.038524	0.041316
25	52	55.295	98.627	43.332	0.037486	0.04407
25	54	59.936	104.53	44.598	0.036882	0.047495
25	56	64.532	110.84	46.305	0.036623	0.051861
25	58	69.118	117.66	48.546	0.036659	0.057644
25	60	73.721	125.22	51.496	0.036961	0.065767

Among the different possible configurations, those with a value of R equal to $25\ mm$ have been discarded, since the range of beta is much smaller compared to the rest of the values. And among the rest of the configurations, the extreme values have been considered.

Therefore, the four final cases to be analyzed in more detail are the following:

- $\boldsymbol{Case\ 1} \rightarrow R\ = 15\ mm\ and\ L = 50\ mm$
- $\boldsymbol{Case\ 2} \rightarrow R\ = 15\ mm\ and\ L = 60\ mm$
- $\boldsymbol{Case\ 3} \rightarrow R\ = 20\ mm\ and\ L = 50\ mm$
- $\boldsymbol{Case\ 4} \rightarrow R\ = 20\ mm\ and\ L = 60\ mm$

Lastly, it can be concluded from the following graphs that the lower the value of L, the more constant the force that the actuator has to exert. Furthermore, in case 2 the mechanism is not valid for the entire linear range and has therefore been discarded. With three possible configurations remaining, we have opted for the configuration of case 3, where the range of beta is sufficient for our wind turbine and also ensures that the force to be exerted by the actuator is as constant as possible.

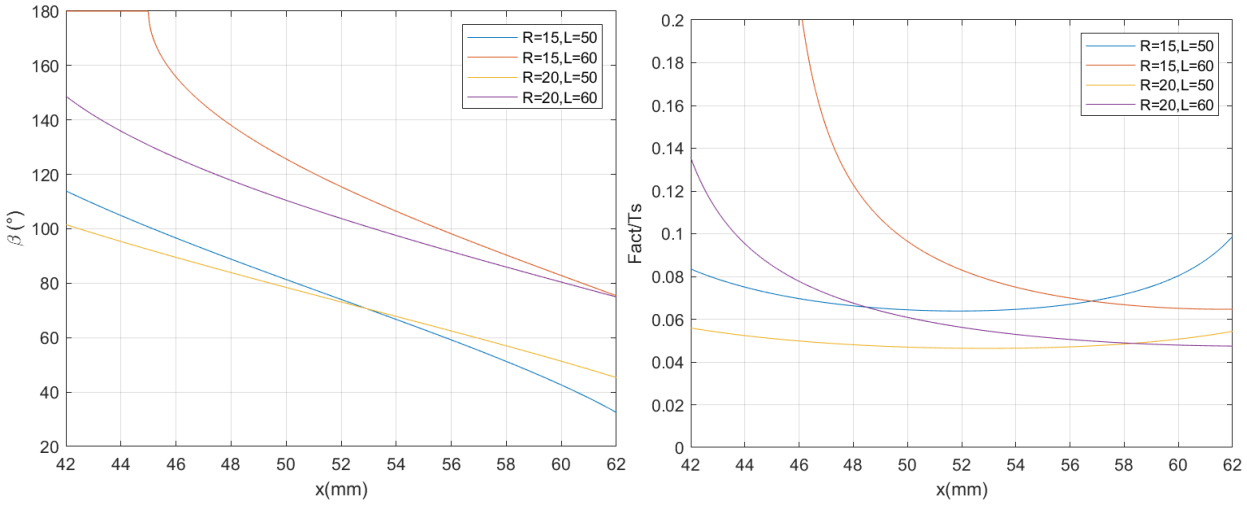

Figure 38 Analysis of the mechanism in terms of linear motion

Plots of the final design of the pitch mechanism have been obtained for the configuration of case 3 (see Figure 39).

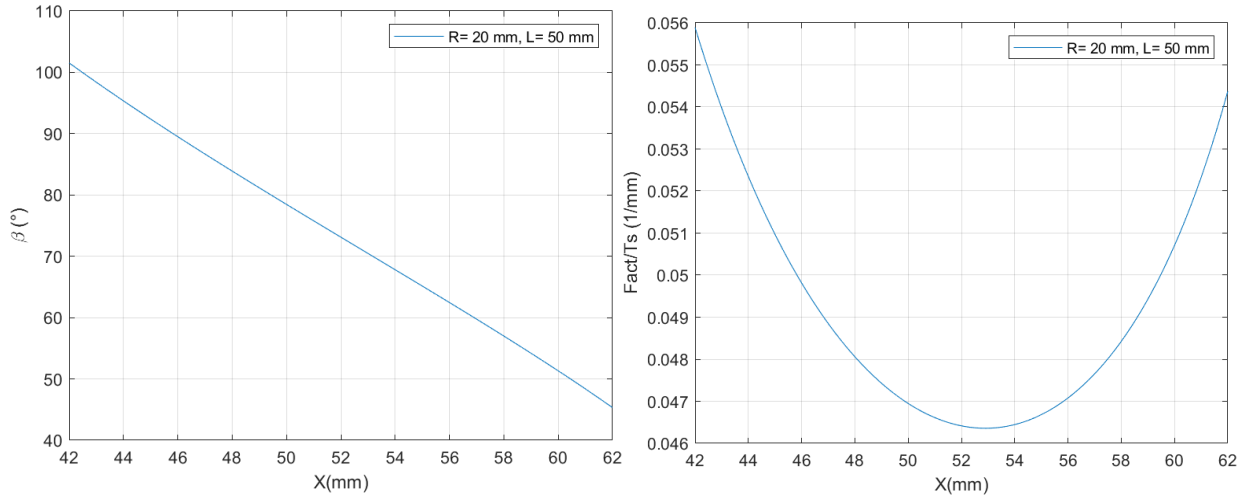

Figure 39 Design values for the chosen configuration (case 3)

Where the most relevant parameter values are detailed below.

Table 3 Final configuration's most relevant parameters

Parameter	Value
R	$20\ mm$
L	$50\ mm$
x_{min}	$42\ mm$
x_{max}	$62\ mm$
β_{max}	$101.54\ °$
β_{min}	$45.314\ °$
$\left.\frac{F_{act}}{T_s}\right\|_{max}$	$0.0559\ \frac{1}{mm}$
$\left.\frac{F_{act}}{T_s}\right\|_{min}$	$0.0464\ \frac{1}{mm}$

Finally, since we are interested in the pitch angle shown in Figure 40, it has been decided that the R-L mechanism and the blade pin will be connected in such a way that when the pitch angle is zero and the beta angle is maximum (reference position).

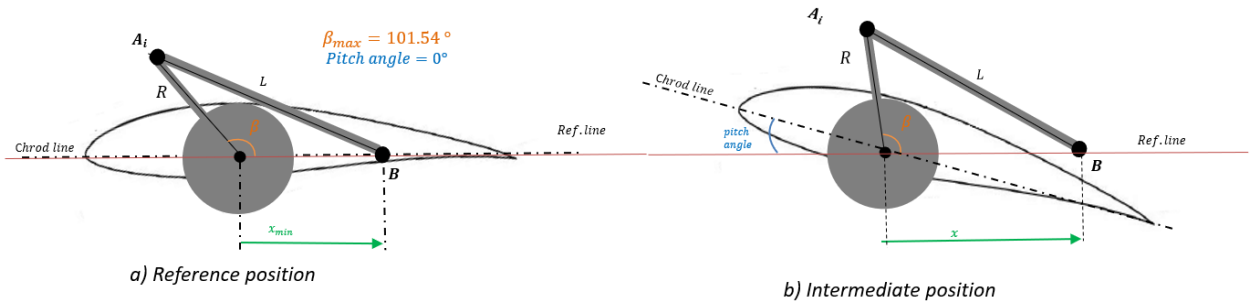

Figure 40 R-L mechanism connection to the blade mountain pin

In the next graph it can be seen the relation between beta and pitch angles through the linear movement.

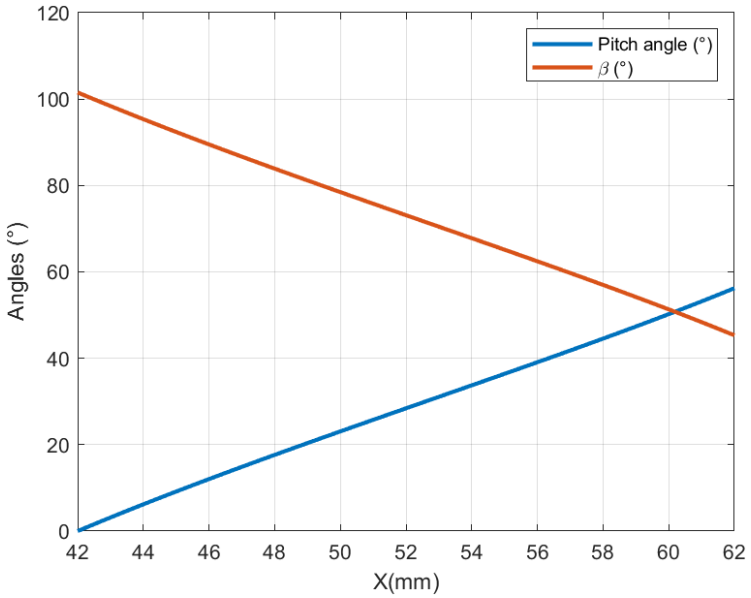

Figure 41 Relation between the pitch angle and beta

4.3. Actuator selection

As we have mentioned before we are looking for a single servo motor for the 3 blades pitch. We also concluded that the design and construction of this mechanism will be much simpler if instead of using rotational movement transmission, as it's used with the gears; we use linear movement, that in the output is transformed into the blade's pitching movement.

As the relationship between the maximum force of the actuator and the torque it exerts on the blades has been obtained (Eq.24) the force to be exerted by the actuator can be calculated. In addition, the resistance torque on each blade is already known from the CFD simulations (Table 1) and has a value of $0.16\ Nm$.

To perform the calculation, a safety factor of 1.5 will be considered, therefore, the final resistance torque to be overcome and the maximum force of the actuator is:

$$T_s = T_R = 0.16\ [Nm]\ \ 3\ [blades]\ \ 1.5 = 0.72\ Nm \qquad 25$$

$$\left.\frac{F_{act}}{T_s}\right|_{max} = \ 0.0559\frac{1}{mm} \rightarrow F_{act}|_{max} = \ 0.0559 T_s = 0.0559\ \left[\frac{1}{mm}\right] 720\ [Nmm] = 40.248\ N \qquad 26$$

Hence, the parameters to be considered for the selection of the linear actuator are as follows:

- The force at least the actuator must exert → $Fact = 40\ N$
- The maximum stroke at least should be → $x = 20\ mm$
- Small dimensions of the actuator

With all this in mind, the selected actuator considering the price/performance ratio is the model PQ12 of the Actuonix miniature linear actuators. One of the advantages of this model is its size and weight. Furthermore, this model has an internal potentiometer that can be used to provide feedback of its position.

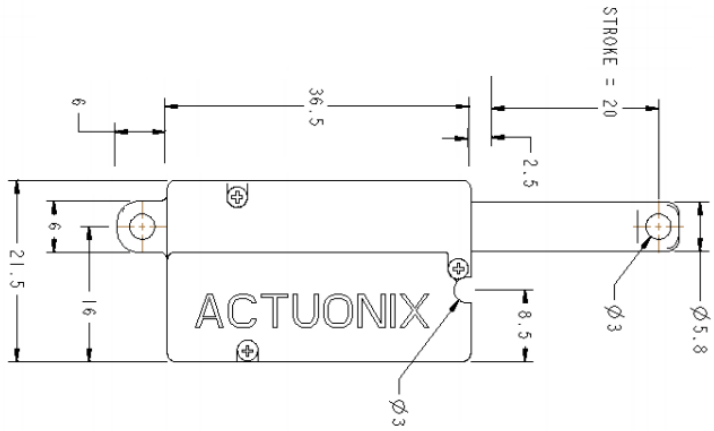

Figure 42 Chosen linear actuator model (Actuonix PQ12)

The main characteristics of the actuator are as follows:

Table 4 Specifications of the actuator (Actuonix PQ12)

Parameters	Value
Gearing Option	100:1
Peak Power Point	40 N @ 6mm/s
Max Force (lifted)	50 N
Max Side Load	10 N
Back Drive Force	35 N
Stroke	20 mm
Input Voltage	6 V
Mass	15 g

4.4. Pitch Mechanism CAD design

As previously mentioned, a crank-crank mechanism has been designed to perform the rotational movement on the longitudinal axis of the blade. This will be connected to the remaining pitch mechanism, which will transmit the necessary force to carry out this rotation and which is exerted by the actuator. In the next Figure 43 a general overview of the mechanism design can be seen.

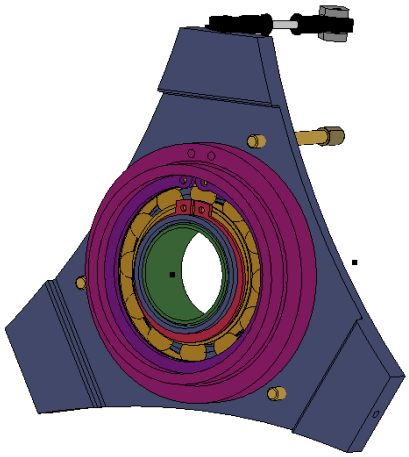

Figure 43 Pitch mechanism overview

The system is based on the fact that the roots of the three blades are joined to a single structure, called pitch disk, which uses the connecting rod-crank mechanism to transform linear displacement aligned with the axis of the shaft into the rotational movement of the blade around its axis. The following Figure 44 shows the essential parts that constitute the pitch mechanism.

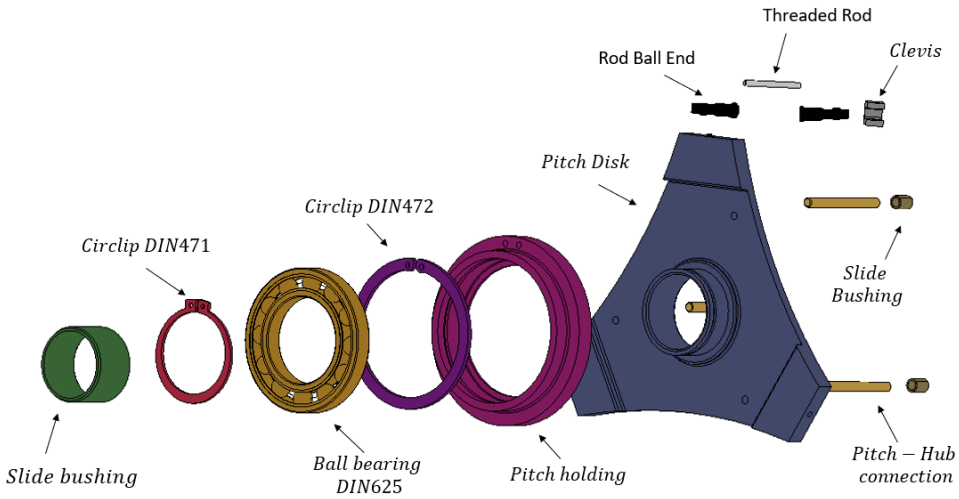

Figure 44 Parts that conform the final pitch mechanism

To describe the designed mechanism, it has been divided into 4 different parts: pitch disc, pitch support, crank mechanism and bearings and each part will be described in detail below.

– **Pitch disk**

This is the central element of the mechanism, it is a rigid body that simultaneously transmits the force exerted by the actuator to the three rod-crank mechanisms connected to the blades. This ensures that the angle at which they rotate is the same for all of them. In the Figure 45 it can be seen the dimensions of the pitch disk.

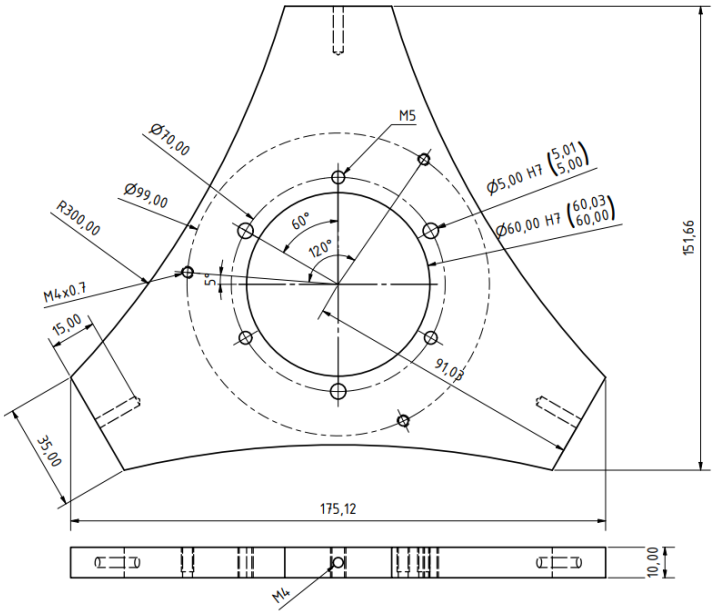

Figure 45 Pitch disk drawing

The pitch disk will perform two movements, it will rotate together with the hub around the shaft thanks to the designed elements that attach it to the hub (pitch-hub connections) that are shown in Figure 46 and it will also perform a linear movement with the rest of the mechanism.

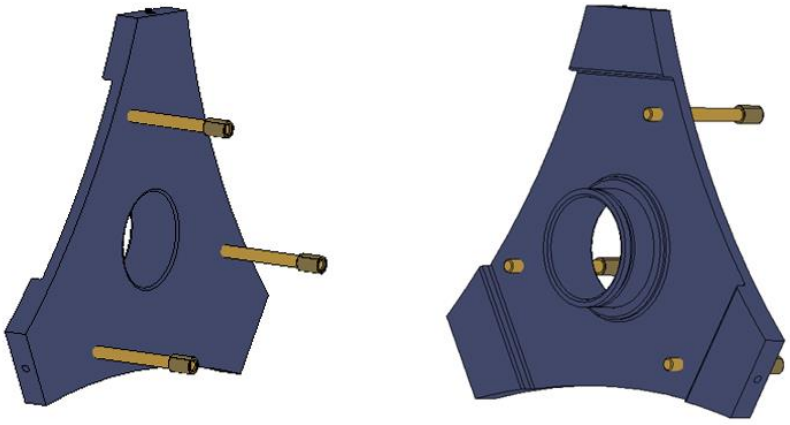

Figure 46 Pitch-hub connections

– **Bearings**

The mechanism is designed with two bearings that allow us to achieve the desired linear and rotational movement: the linear bearing or bushing slide (green) which is connected directly to the shaft and the ball bearing (orange). The combination of these two bearings is responsible for rotational movement fixed to the shaft and enables the linear movement along it.

In addition, the ball bearing prevents the pitch holding from rotating as it is directly connected to the actuator and therefore it must only perform the linear movement. The bearing is connected to the pitch disk and holding by circlips as shown in the next figure.

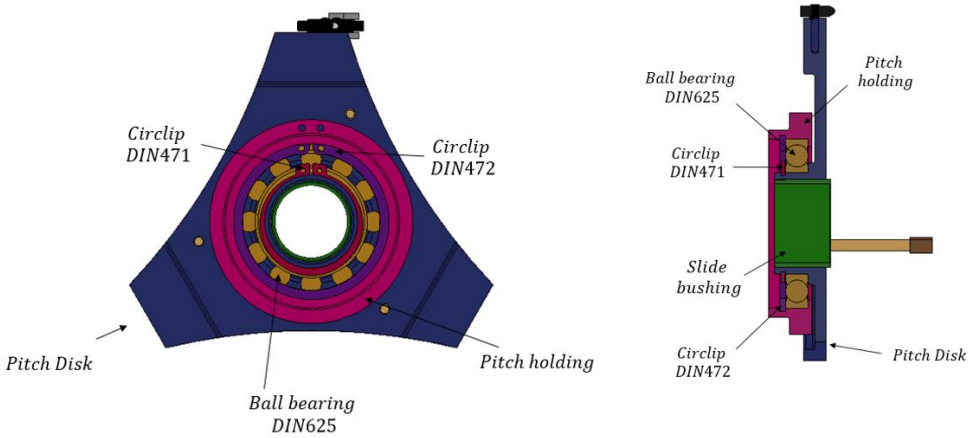

Figure 47 Pitch mechanism front and half section view

– **Pitch holding support**

As we have already said this element is directly attached to the ball bearing and at the same time is connected to the servo motor, which will provide the necessary force for linear movement. In the Figure 48 it can be seen the dimensions of the pitch holding and in the upper part there can be noticed two holes that will be used to fix the actuator to the mechanism.

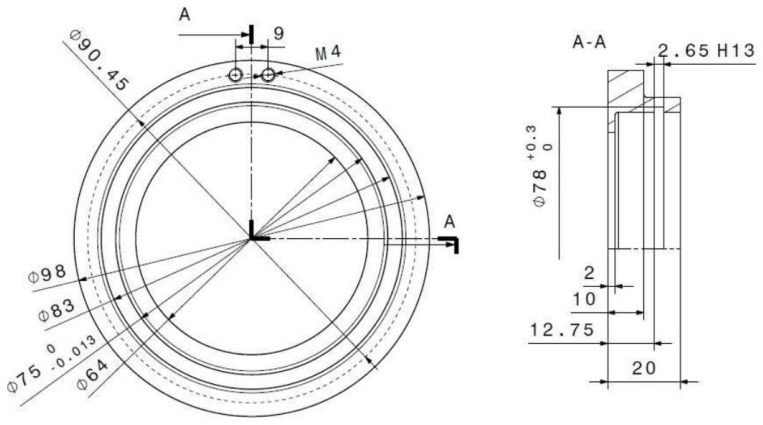

Figure 48 Pitch holding drawing

To make the connection between the actuator and the pitch mechanism, a connecting piece and a pin have been designed to be attached to the actuator which is located inside the nacelle (see Figure 49).

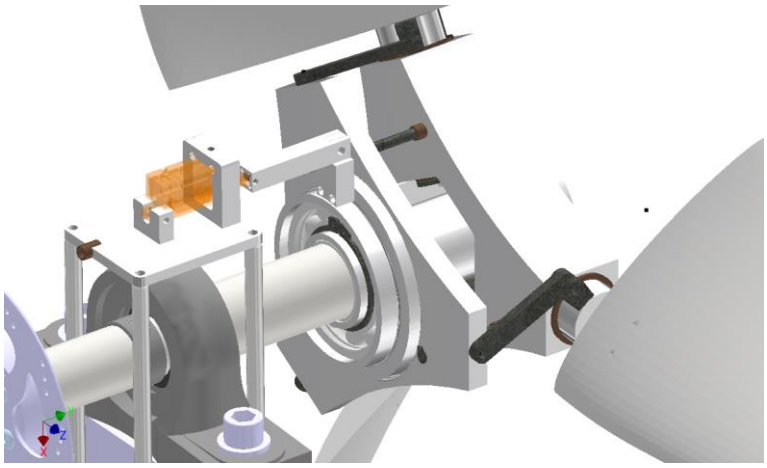

Figure 49 Actuator and pitch mechanism connecting pieces

– **Crank- lide (R-L) mechanism**

This is the element which transforms the linear movement exerted by the actuator into the rotational movement of the blades. It is composed of a threaded rod, two rod ball ends and a clevis that connects the mechanism to the mounting pins.

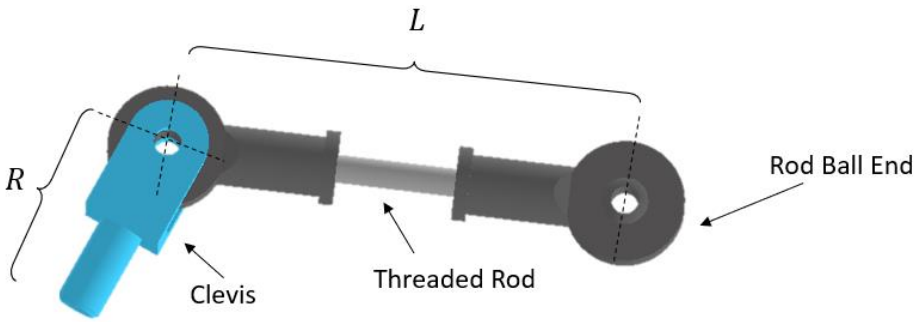

Figure 50 Crank- Slide (R-L) mechanism

The Figure 51 shows the connections that will be made to the wind turbine blade pin.

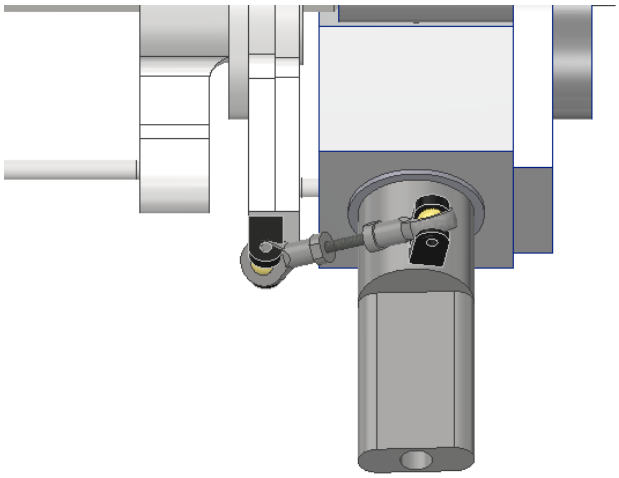

Figure 51 Connections between the pitch mechanism and the blade pin

To conclude, in the following Figure 52, it can observe an overview of the pitch mechanism mounted in the wind turbine.

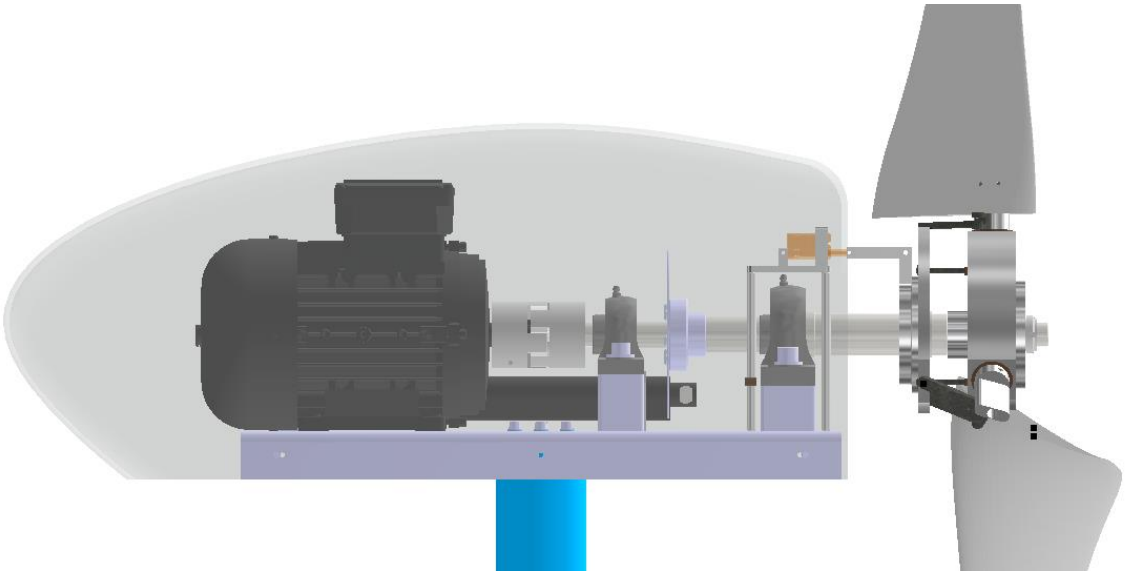

Figure 52 Overview of the pitch mechanism in the Wind Turbine

4.5. Manufacturing and construction of the pitch mechanism

Once the design has been made, it is time to manufacture and purchase the necessary parts. For this purpose, the University of Applied Science Emden/Leer has a workshop where the parts can be manufactured and where material and tools are available to work with.

The main place where the manufacturing and assembly of the mechanism will take place is the FabLab at the university. It is a place that has been available since 2018 for students to carry out different projects. There it can be found different electrical and mechanical tools and some Prusa 3D-Printers (see Figure 53).

Figure 53 Prusa 3D printers available in the FabLab

In Table 5, all the elements that have been used for the assembly of the mechanism and the units that have been needed of each element are detailed, as well as whether it is necessary to purchase or manufacture them.

Table 5 Pitch mechanism part list

Manufactured (m) or purchased (p)	Element	Dimensions	N°
p	Cylindrical plain bearing	35x39x25	1
p	Ball bearing 16009	45x75x10 mm	1
p	Circlips DIN 472	75 - 2.5mm	1
p	Circlips DIN 471	45 - 1.75mm	1
p	Rod Ball End	M3	6
p	Threaded rod	M3	1
m	Pitch holding	--	1

Manufactured (m) or purchased (p)	Element	Dimensions	N°
m	Pitch disk	--	1
m	Clevis	--	3
m	Connection pitch hub	--	3
p	Slide Bushing	SKF PCM 050710	3
p	Screw	DIN 933- M3 x 16	3
p	Bolt	DIN 933- M3 x 16	3

Due to the manufacturing times and the date of the competition, it was decided to make a prototype of the mechanism printed on the 3D printer so that it could be ready for the competition and be able to present it.

The use of the 3D printer available in the FabLab has allowed us to obtain the mechanism in a very short time, which is why the initial design of the mechanism has been adapted in order to be able to print it on the 3D printer. As we can see in Figure 54, the most significant changes correspond to the two main elements of the system: pitch holding and pitch disk, as these are the elements that were to be manufactured in the work shop and which had geometries that do not help to be printed on the 3D printer. The main difference is that the elements have rounded sides which helps to print them and they also need less material which shortens the printing times.

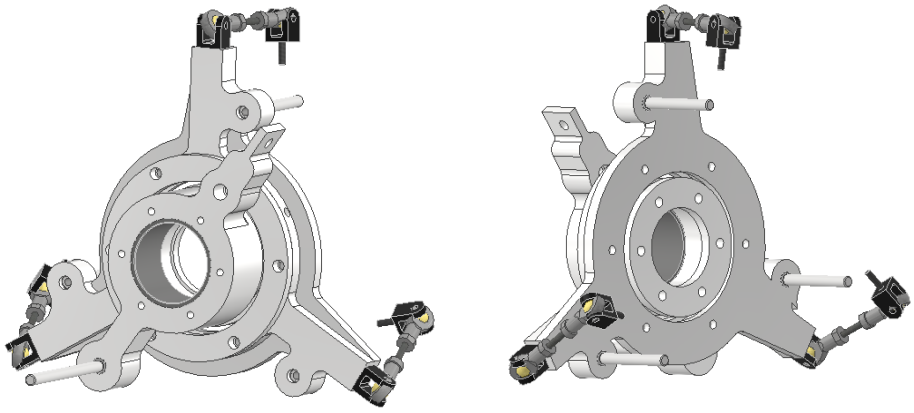

Figure 54 Design of the pitch mechanism prototype

In addition, Figure 55 also shows the prototype of the mechanism in the wind turbine assembly.

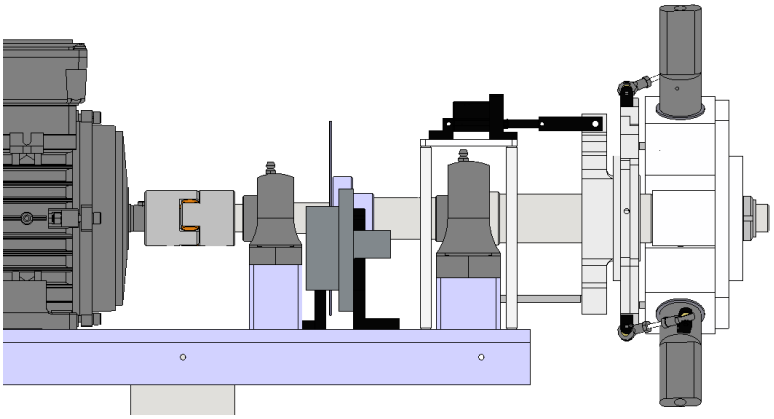

Figure 55 Pitch mechanism prototype overview in the wind turbine

The main parts of the mechanism have been manufactured with the Prusa 3D printer, this will provide us with a first prototype of the mechanism before manufacturing them in aluminium in the workshop at the university. The material used in this printer is PLA and in the Table 6 can be seen the properties of this material.

Table 6 Material properties PLA

Property	Value
Young modulus [E]	2346,5MPa
Poisson ratio [υ]	0.4
Density [ρ]	1240 kg/m³
Tensile strength [TS]	48MPa

The prototype of the assembled mechanism manufactured can be seen in the following Figure 56.

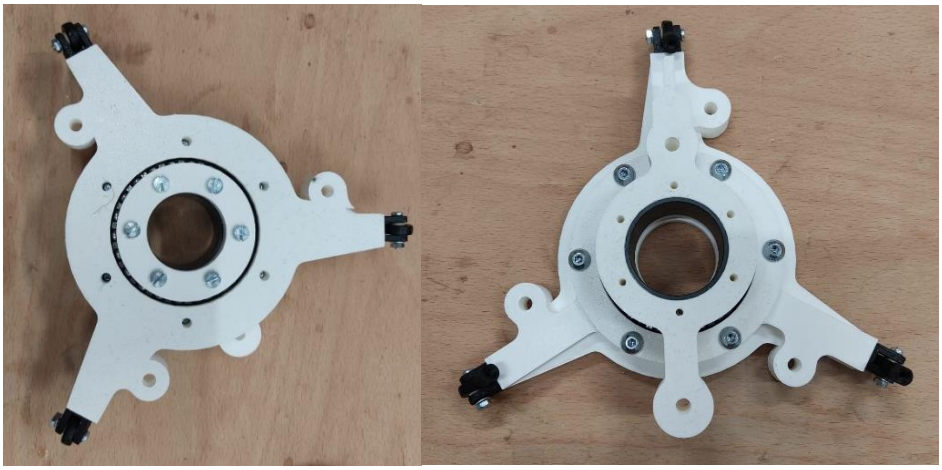

Figure 56 Front and back side of the manufactured mechanism.

Finally, Figure 57 shows the mechanism mounted on the shaft.

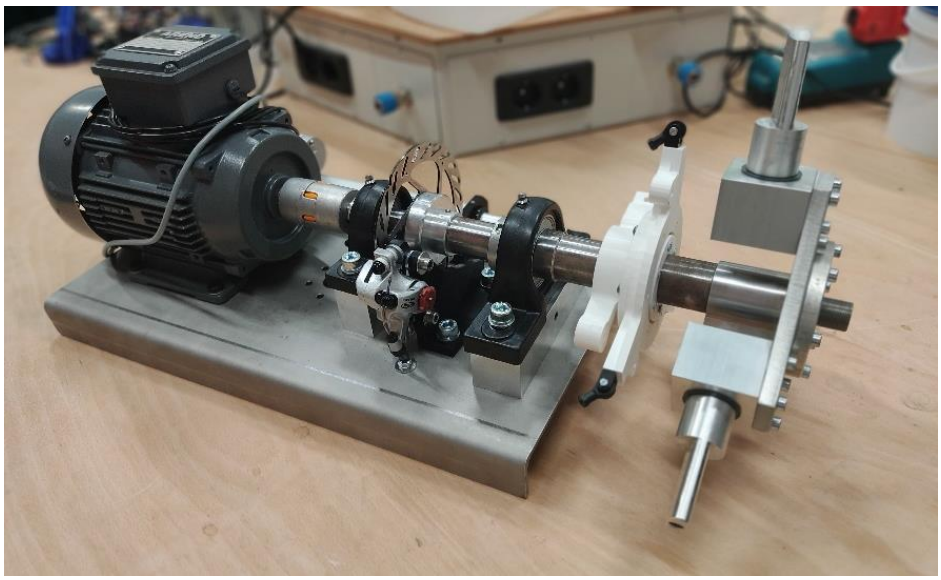

Figure 57 Prototype mechanism mounted on the shaft.

5. Control system

A control system is the set of devices responsible for coordinating, directing, and regulating the behaviour of another system, in order to obtain the expected results and reduce the probability of failure.

In a control system, all the following variables can be identified as having a relevant role in the control system, known as significant variables [23]:

- **Controlled variable:** the system variable whose behaviour is to be controlled.
- **Control signal:** variable that is externally modified to achieve the objective.
- **Disturbance:** its variation influences the controlled variable but is not manipulated.

In addition, the elements to be used in the system will be the following:

- A **sensor** in charge of measuring the controlled variable of the system to be controlled at a certain moment in order to send the feedback signal to the controller.
- A **controller** that will use the data obtained by the sensors to determine the output action of the system.
- An **actuator** that is responsible for executing the output or control command by the controller.

According to the control strategy we want to implement, we can distinguish two types of control systems:

Open loop or no-feedback systems

In an open-loop system the controller will determine the output action only as a function of the input to the control system. In this case, the output has no effect on the control system. Most of these systems will be automatisms, very limited in making intelligent decisions, as they have no way of knowing the results of their previous decision [23]. An example of an open loop control system is shown in Figure 58.

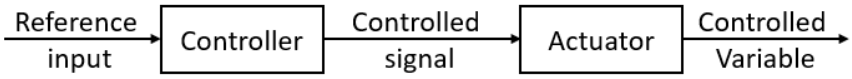

Figure 58 Open-loop control system diagram

Closed-loop or feedback systems

In such systems, the output signal is returned to the control system via the sensors. In this case, the controller will determine the output action based on the error, which is the difference between the input signal and the output signal (feedback). This system is more flexible and will be able to react to expected results. We can see its schematic in Figure 59.

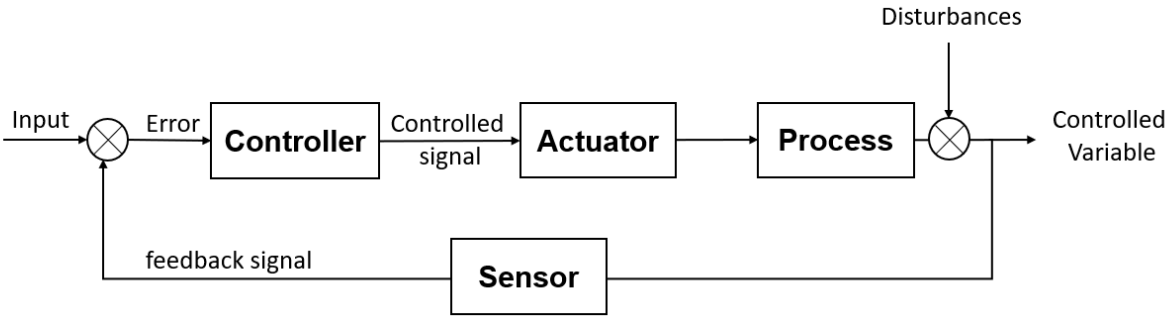

Figure 59 Closed-loop control system diagram

In the current project context, the final objective of the control system will be to implement a closed-loop system that will be responsible for obtaining the desired pitch angle.

From the previous figure, we can identify the following elements in them:

- **Reference signal**: this corresponds to the desired pitch angle or setpoint.
- **Output signal** or controlled variable: in this case, it will be the actual position at which the actuator is at a given moment.
- **The potentiometer**: is an internal element of the actuator that will send the feedback signal to the controller at all times.
- **Controller:** which will be used to take the appropriate decision for the correct operation of the system. The decision will vary depending on the error signal received by the controller.
- **Actuator:** it will be in charge of executing the order of the controller. In our case, it will correspond to the linear actuator that was selected in section 4.3.

5.1. Closed-loop control system types

In the following sections, the two most common types of closed-loop control systems will be described. The first one will be an On/Off type control system and the second one a PID type control system. Depending on the degree of control required in the system to be controlled, one or the other is usually used.

5.1.1. ON/OFF control system

The simplest closed loop control system that can be found is the ON/OFF control system. This control will only offer two possible output states, a fully ON state (100% ON) or a fully OFF state (100% OFF). One state will be used when the measured position is below the setpoint position and the other when the measured position is above the setpoint position [24].

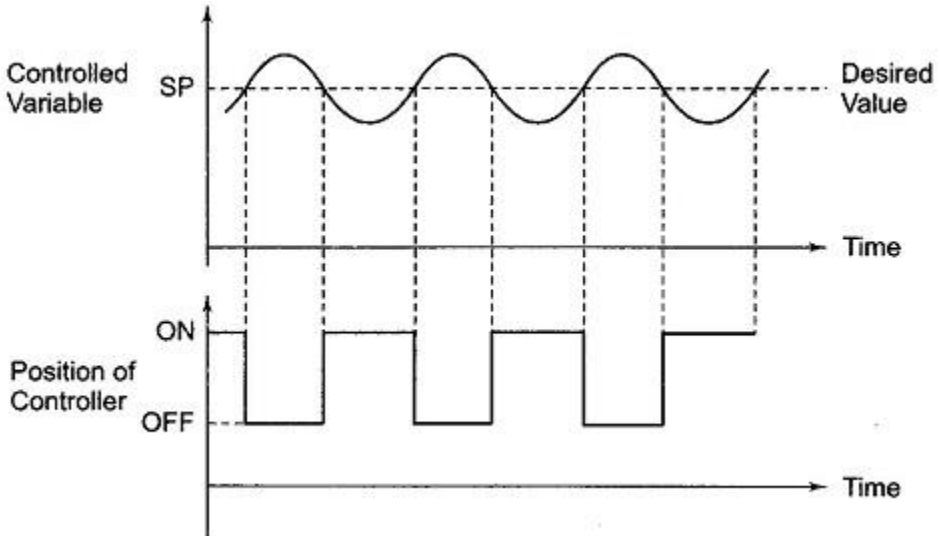

Figure 60: ON/OFF control system performance over time. [25]

As can be seen in Figure 60, the ON/OFF type control system presents two problems:

1. The first problem will be that the position will oscillate, since the measured position must cross the set point for the controller to act.
2. The second problem will be the occurrence of overshoot and undershoot. The overshoot will be the extent to which the measured position exceeds the set point until the controller acts. The undershoot shall be the opposite.

During the design of these control systems, the aim is to reduce as much as possible this oscillation as well as the overshoot and undershoot. For this purpose, a hysteresis range is usually defined, which will measure the sensitivity of the controller. This means that the controller will only work when the difference between the measured position and the setpoint position is over the defined hysteresis range.

5.1.2. PID control system

A proportional, integral and derivative control system, namely a PID control, is used in situations where a more precise control system is required. Like the On/Off system, it can be a closed-loop control system. However, the PID control system implements an algorithm that combines the action of three types of control, time proportional control, integral control and derivative control. Each of them provides a higher precision to the PID controller. In Figure 61, we can visualise the schematic of a PID control system.

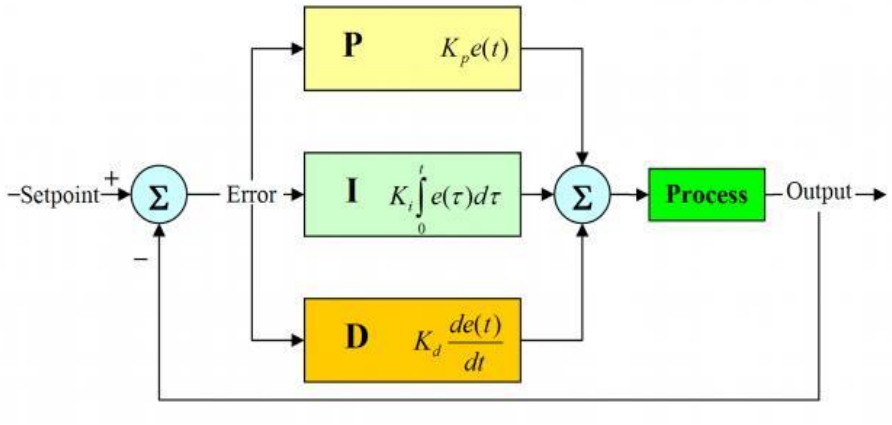

Figure 61: Diagram of the elements of a PID-type controller [26]

The main objective of the PID controller will be to reduce the steady-state error to zero, i.e. the difference between the setpoint position (input signal) and the measured position (output signal). In addition, it will try to solve the two problems that appear with On/Off type control systems, i.e. the occurrence of "overshoot" and "undershoot" and the oscillation of the measured position.

As previously mentioned and as can be seen in the Figure 61, the PID controller combines the action of three controllers. These controllers will be the following [27]:

5.1.2.1. Proportional control (P)

In proportional control, the controller output is proportional to the input error signal. Therefore, the response of this control will be instantaneous to any variation of the error [28].

$$Y(t) = K_p\, e(t) \qquad 27$$

As we can see in the formula, the output signal will be the result of the product of the error signal and the proportional band or constant K_p. Therefore, as we increase the value of K_p, we increase the system response and reduce the steady state error.

While increasing that value, there will be more overshoot. In addition, if a small value for K_p is chosen, the controlled system will oscillate as in the case of the On/Off control. Figure 62 shows an example of the effect of varying K_p in a PID controller.

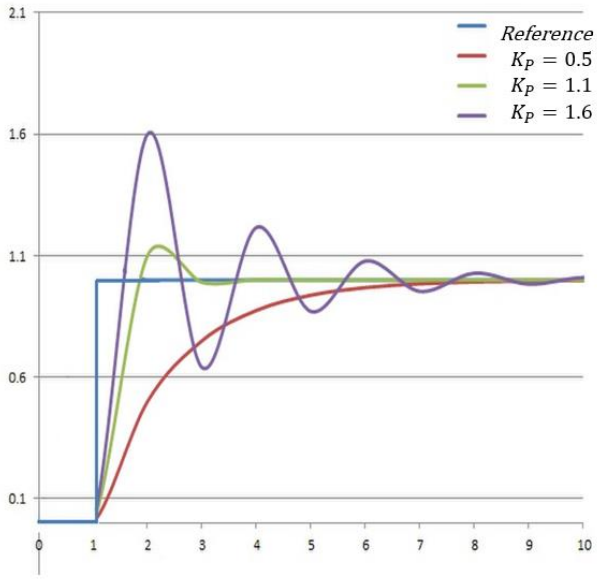

Figure 62: Example of a performance of a proportional control system as a function of the value of the proportional constant K_p over time. [27]

5.1.2.2. Integral control (I)

In the integral control the output of the controller is proportional to the accumulated error over time. The objective of integral control shall be to reduce and eliminate the small error after proportional control. For this purpose, integral control shall follow the following formula:

$$Y(t) = K_i \int_0^t e(t)\, dt \qquad 28$$

As we can see the control action will result from the product of the integral constant K_i by a summation of the error obtained in a given period. Due to this integration, even the smallest possible error will cause a small increase in the integral control output signal. Therefore, the control output signal will increase until the error is zero.

However, as we increase the value of the proportional constant K_i, the system response will become more oscillatory and may become destabilised.

As we saw earlier, it will take some time for the controller action to be noticed at the output of the system. The derivative action will try to anticipate this change, it is based on introducing a predictive action on the error signal. The formula that follows this action will be: Figure 63 it can be check an example of the effect of the variation of K_i in a PID controller.

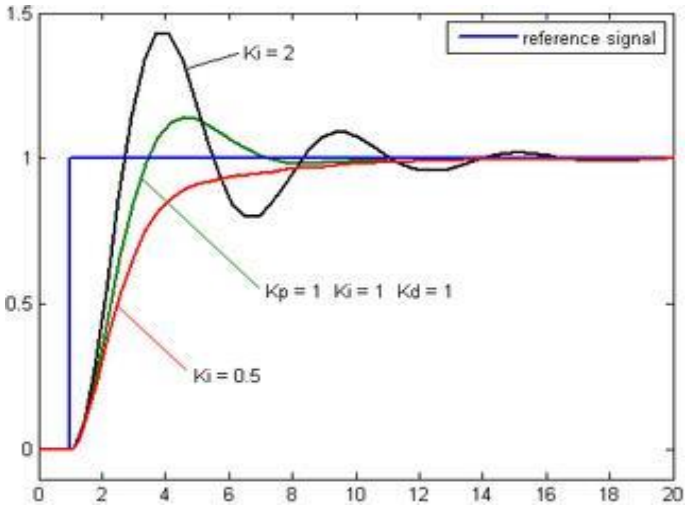

Figure 63: Example of the performance of an integral control system as a function of the value of Ki over time. [27]

5.1.2.3. Derivative control (D)

The aim of this control is to improve the stability of the system by correcting the possible overshoot and undershoot still present after the proportional and integral action. And it will take some time for the controller action to be noticed at the output of the system. The derivative action will try to anticipate this change, it is based on introducing a predictive action on the error signal. The formula following this action is:

$$Y(t) = K_d \frac{\partial e(t)}{\partial t} \qquad 29$$

As we can see, obtaining the derivative of the error over a period of time tells us the instantaneous change in the control action. If we increase the value of the derivative constant K_d, our system will have a faster reaction to changes in the error signal, and we can reduce it before it becomes too large.

However, a small value for the K_d constant is normally used, as the derivative action is sensitive to noise. So, its value must be chosen carefully, because if the signal fed back by the sensor introduces noise and the control system has a high response time, a high value of K_d can saturate or destabilise the system. Figure 64 shows an example of the effect of varying K_d in a PID controller.

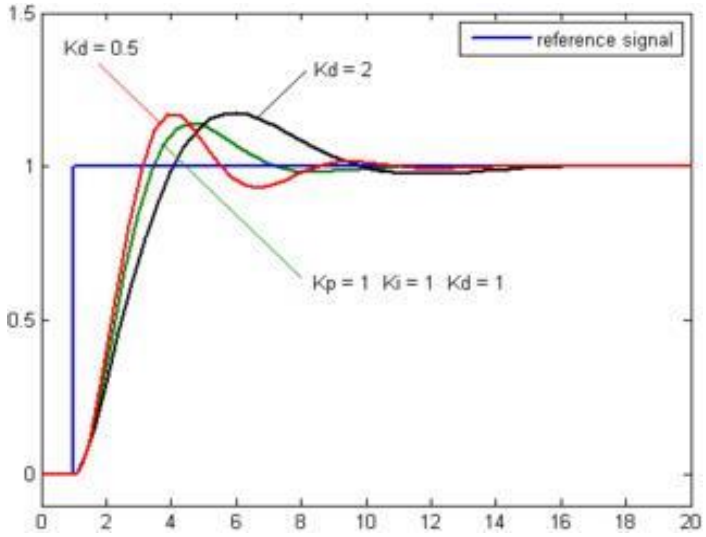

Figure 64: Example of the performance of a derivative control system as a function of K_d over time. [27]

As we have seen, the combined action of proportional, integral and derivative action form the PID controller. This controller is the most widely used for any industrial control application, as the degree of control it offers is quite high and sufficient for most applications. In equation 30 we can see the formula that the PID controller follows:

$$Y(t) = K_p\, e(t) + K_i \int_0^t e(t)\, dt + K_d \frac{d\, e(t)}{dt} \qquad 30$$

However, as we saw in previous sections corresponding to proportional, integral and derivative action, the values of the constants K_p, K_i and K_d must be carefully chosen for the control system to work properly.

5.2. Control system components

The operation of the pitch mechanism will be controlled by the Arduino Nano and the actuation and transmission systems, as we have already seen, are composed of the linear actuator PQ12 and the pitch mechanism. Figure 65 shows the distribution of the elements of the complete system according to their function.

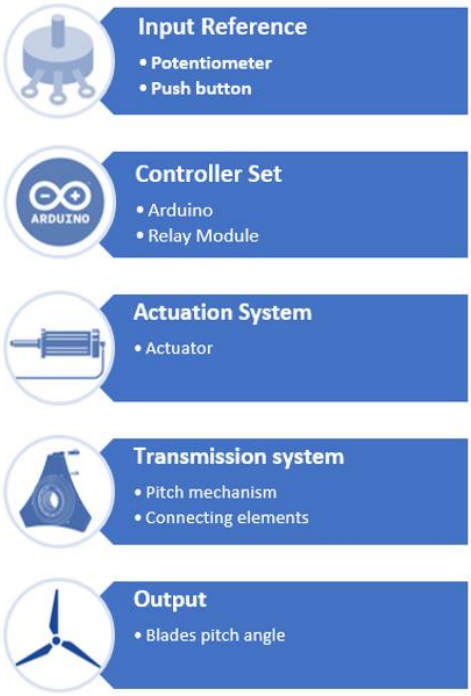

Figure 65 Scheme of the system elements according to their function

The elements used in the system and the connections are presented below.

5.2.1. Actuator

The actuator that will be used, as mentioned in section 4.3, is the PQ12 which has an integrated potentiometer to determine the position of the piston at any time (see Figure 66).

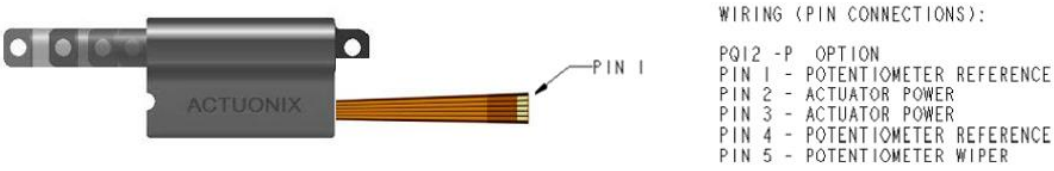

Figure 66 Actuonix PQ12 Pins

Figure 67 shows the different connections that have been made, as we have seen in Figure 66 the actuator has five pins: two pins (1 and 4) are used to power the actuator and will be connected to the relay module which enables the extension or retraction of the piston. The remaining pins correspond to the internal potentiometer, where two of them will be used as a reference for the data pin (pin 5) in order to send the exact position to the Arduino.

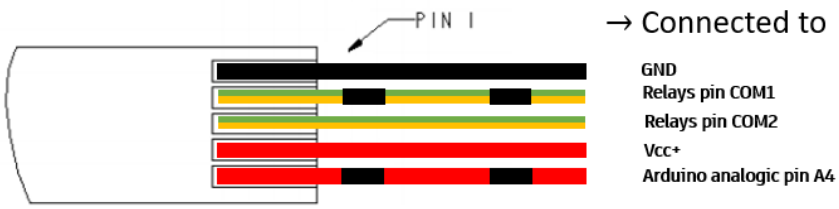

Figure 67 Actuator wiring connections

5.2.2. Arduino Nano

With the Arduino platform we can develop our own electronic projects, with a series of inputs, such as sensors or buttons, we can control different output devices, whether they are lights, motors or various electronic devices [29]. Furthermore, Arduino programs can be autonomous, so if the board, once programmed, does not need to be connected to a computer and works independently.

In this project we are using the Arduino Nano board that is one of the smallest development boards that the Arduino brand works with, with dimensions of $18.5x43.2\ mm$ and a weight of $5g$, good data for implementation in a small wind turbine [29].

The hardware consists of a printed circuit board with a microcontroller, and input/output ports, which can be connected to other modules that increase the functionality of the board.

This board incorporates the ATMega328P microchip, which makes it maintain similar features to the Arduino UNO in terms of speed and types of signals, differing mainly by the number of possible pins to connect. As for its power supply method, it is via a Mini-B USB connector.

Figure 68 Arduino Nano

Table 7 details the characteristics of the Arduino Nano board [29].

Table 7 Main characteristics of Arduino Nano

Microcontroller	ATmega328
Architecture	AVR
Operating Voltage	5 V
Flash Memory	32 KB of which 2 KB used by bootloader
SRAM	2 KB
Clock Speed	16 MHz
Analog IN Pins	8
DC Current per I/O Pins	40 mA (I/O Pins)
Input Voltage	7-12 V
Digital I/O Pins	22 (6 of which are PWM)
PWM Output	6
Power Consumption	19 mA

As mentioned above, there are a total of 22 analogue and digital pins but for this project it will be only used the pins shown in Figure 69 .This board will be located in the control box.

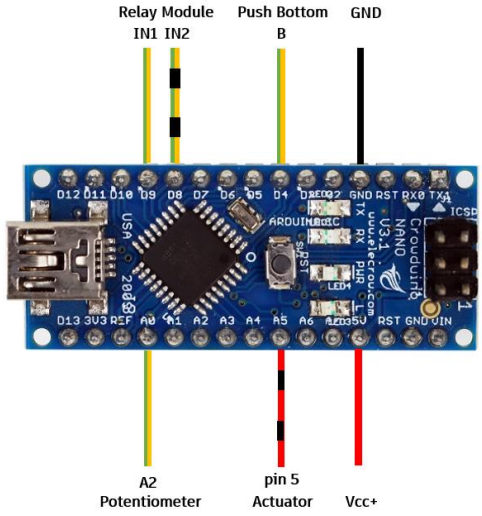

Figure 69 Arduino Nano pins connections

5.2.3. Channel Relay module

The relay is the device that will be used to control the direction of rotation of the linear actuator, since the polarity of the voltage on the actuator supply pins must be reversed to extend or retract the piston. The relay module shown in Figure 70 is used for this purpose. It will be located in the control box, as well as the Arduino Nano.

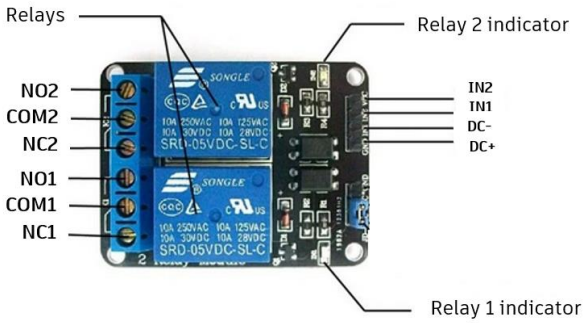

Figure 70 Relay module schematic

The main parts are:

- **Connection pins (IN1 and IN2):** used to connect the relay to Arduino.
- **Terminals (COM1 and COM2):** used to connect the device to be controlled by the relay.
- **Green LED (activation):** lights up when the relay is active.
- **Red LED (power):** lights up when the relay is powered.

Figure 71shows the connections made.

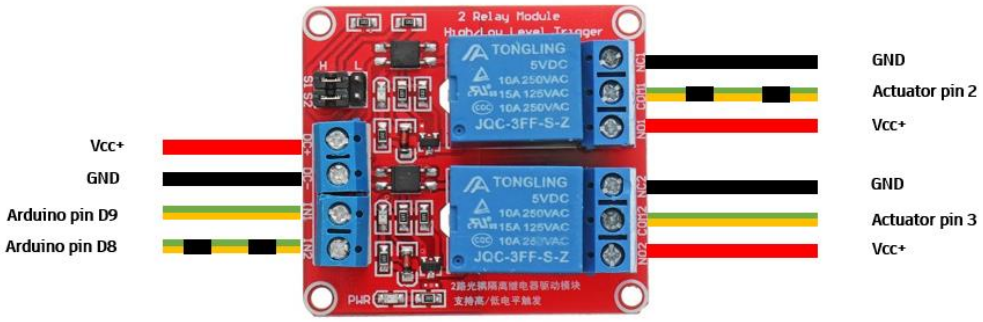

Figure 71 Relays module wiring connections

5.2.4. Push button

A pushbutton has also been included so that the actuator moves to the position indicated by the potentiometer when it is pressed. In the Figure 72, it can be seen the connections made.

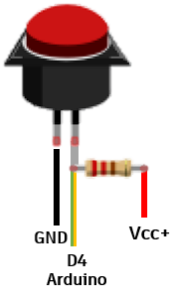

Figure 72 Push button wiring connections

Digital pin produces a binary output signal whose logic: 1 represents a voltage of 5V and its logic 0 represents a voltage of 0V. A digital signal does not produce continuous values, but discrete values. Compared to analogue signals, they are significantly more accurate, as a digital signal is not as affected by noise. Furthermore, the precision of a digital signal will depend on the number of bits that are used to represent the measured value.

To prevent excess current from the circuit from reaching the microcontroller, resistors called "pull-down" and "pull-up" resistors are used to prevent any button from being connected to a microcontroller. To understand the use of both resistors, let's consider the example of a push-button with two states, "on" and "off". As we can see in Figure 73, if we place a pull-up resistor for the pushbutton, when the pushbutton is open, the current flow will circulate through the input pin to the microcontroller offering in the digital signal a logic 1.

Conversely, when the pushbutton is pressed, it will be closed, so the current flow will be directed to ground, indicating a logic 0 on the microcontroller input pin in the digital signal. On the other side, in case of connecting the resistor in "pull-down" mode, when the push-button is pressed, the digital input signal to the microcontroller will have a logic 1 and when it is not pressed it will have a logic 0.

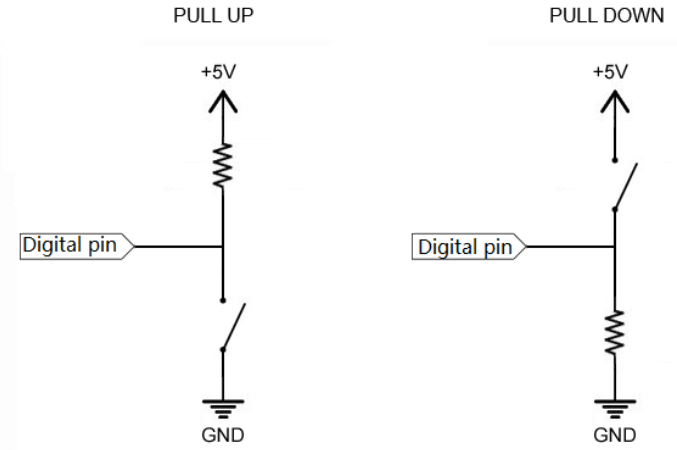

Figure 73 Pull-up and pull-down resistors [29]

5.2.5. Potentiometer

The potentiometer is connected to a circuit in such a way that it will output a specific voltage range, typically between 0 and 5V, i.e. it produces an analogue output signal, continuous in time and amplitude. This analogue output signal is routed to an analogue input pin on the microcontroller which uses an analogue to digital converter to convert the sensor output voltage into a numerical value that we can read and process further.

In the case of our Arduino Uno, each analogue pin has an analogue-to-digital converter with a 10-bit resolution, i.e. it gives us a range of numerical values between 0 and 1023, with 0 being the lowest value in the voltage range (0V) and 1023 being the highest value (5V).

The potentiometer used is rotational type and is used as an input element to enter the desired pitch angle manually. The following figure shows the cable connections to the other elements of the system.

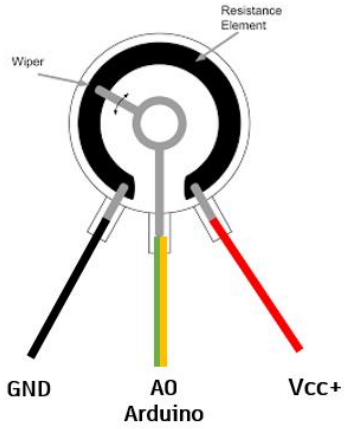

Figure 74 Potentiometer wiring connections

The relationship between the potentiometer input and the analogue signal it sends to the Arduino board is linear and is shown in Figure 75. The input data range of the potentiometer varies between 0 and 7.8 in steps of 0.2. So, in total there are 40 different positions that will be translated into an analogue signal between 0 and 1023.

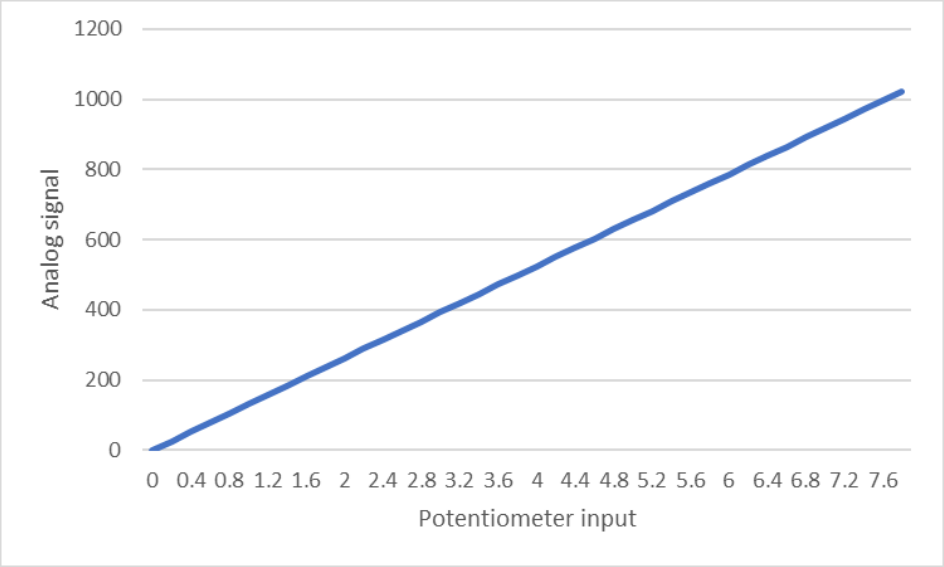

Figure 75 Potentiometer input-analog signal relation

Finally, the following Figure 76 shows the relationship between the input values of the potentiometer and the pitch angle resulting from the control.

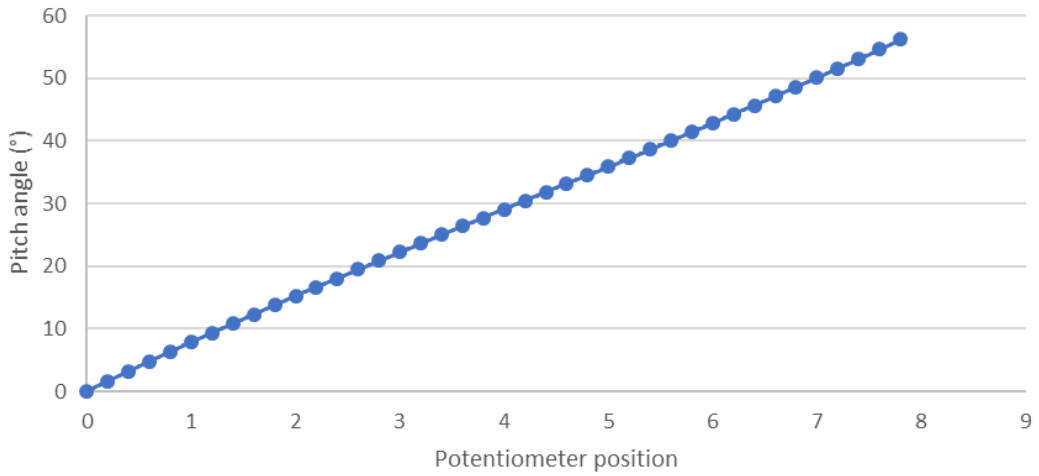

Figure 76 Relationship between the potentiometer input and the pitch angle

To determine this relationship, we started from the previous relation shown in Figure 75 and related this data to the values obtained in Figure 39, which connects the position of the actuator to the beta angle. In addition, to obtain the final relationship with the pitch angle, a change has been made using the correlation shown in Figure 40 and used to obtain Figure 41.

5.3. Software implementation

This chapter describes the software implementation of the control system. Firstly, the mechanism position control will be developed with the first of the types of closed-loop control systems explained in section 5.1.1: ON/OFF control system. This system is a first approximation to the desired final objective. Once this control system has been developed, it will be analysed whether its performance is sufficient for this particular application or another type of control has to be implemented.

5.3.1. Pitch mechanism position control

In this section, it will describe the position control performed on the pitch mechanism designed in previous sections. The main objective of this control is to move the mechanism to a certain position so that the mechanism rotates the pitch to the desired angle.

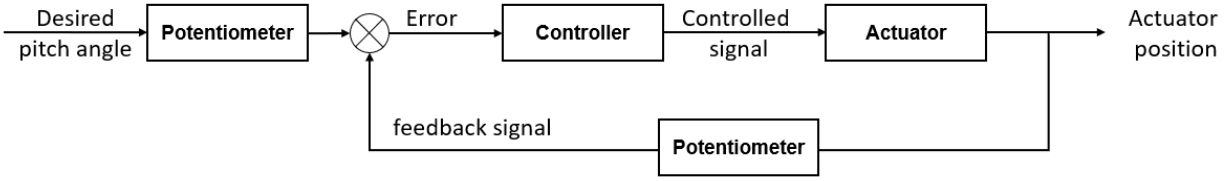

Figure 77 Pitch mechanism position control diagram

As can be seen in the previous Figure 77, the operation of this control will be as follows: the desired pitch angle will be entered manually by means of a potentiometer and the controller, depending on the position in which the actuator piston is located, will decide whether to switch on the relays and, if so, which one to switch on. Depending on which relay is switched on, the actuator will be retracted or extracted, moving it to the desired position. In addition, the actuator's internal potentiometer will send the actual position of the actuator at any given moment.

In the previous section 5.2, the connections between the elements of the system have been detailed and in the next table shows where each element will be located.

Table 8 Control elements location

Component	Location
Actuator	Nacelle
Arduino	Control box
Relay module	Control box
Push button	Nacelle external box
Potentiometer	Nacelle external box

As previously mentioned, the control will be performed by Arduino and therefore it is necessary to program the code that will be executed in the controller. The programming code is described and shown below and can be differentiated in four main blocks:

– **Part 1:** Variable declaration

First of all, the parameters that determine the pin to which the elements of the system are connected to the Arduino board have been defined. These will be constant parameters, i.e. they will not be modified during the code (see Figure 78). The second part of this block contains the internal variables of the system that will take different values as the code is executed. Figure 78 shows the role of each of the variables.

```
// constants won't change. They're used here to set pin numbers:
const int buttonPin = 4;       // the number of the pushbutton pin
const int relay1Pin =  6;      // the number of the Realy1 pin
const int relay2Pin =  11;      // the number of the Relay2 pin
const int actuarorPotPin = A5; // the number of the Actuator Wiper pin
const int potPin = A0;          // the number of the external potentiometer reference
const int emergencystop= 5  // the number of the emergencyStop pin

// variables will change:
int buttonState = 0;         // variable for reading the pushbutton status
int actualposition =0;        //lecture of the actuator potenciometer
int potlecture=0  ;             //lecture of the external potentiometer
int goalposition =0;          // variable to save the goal position of the actuator
int maxmintolerance= 35;   //tolerance of the position
```

Figure 78 Arduino code part 1: Variable declaration.

– **Part 2:** Single Run Setup

The second block of the code is where the criteria that require a one-time execution have been established. Since in this maser thesis we will need to visualise certain variables to know if the controller is working as we want, we will execute the serial communication using the "Serial.begin" command.

In addition, in this block we will also determine the type of pins defined in the previous block: input or output. For this we use the "pinMode" function. Generally, all the pins are configured as input pins, but it is advisable to define all of them to avoid making mistakes.

```
void setup()
{
  Serial.begin(9600);
  // initialize the pushbutton pin as an input:
  pinMode(buttonPin, INPUT);
  pinMode(emergencystop, INPUT);
  // initialize the relay pin as an output:
  pinMode(relay1Pin, OUTPUT);
  pinMode(relay2Pin, OUTPUT);
  potlecture  = analogRead (potPin);
  goalposition = potlecture;
}
```

Figure 79 Arduino code part 2: Single Run Setup

– **Part 3:** Main program (Loop)

This third block corresponds to the main function of the program. It is the part of the code where the commands that will be executed while the Arduino board is enabled have been written. Starting with the first command, the microcontroller will go to the end and immediately jump back to the beginning to repeat the same sequence. And so on for an infinite number of times (as long as the board has power supply).

The operation of this code block is as follows: first, a line has been defined so that the code is executed when the emergency stop is not active. If this condition is met, the system will read the values of both potentiometers and display them in the serial communication started in the previous block. In this way, we will be able to visualise the position of the actuator at the given target position at all times.

Finally, several *if* loops have been used to determine whether the actuator piston will extend or retract. Also tolerance has been defined for the actuator to stabilise when it is close to the target position. In Figure 80 the controller decision-making block diagram can be visualised.

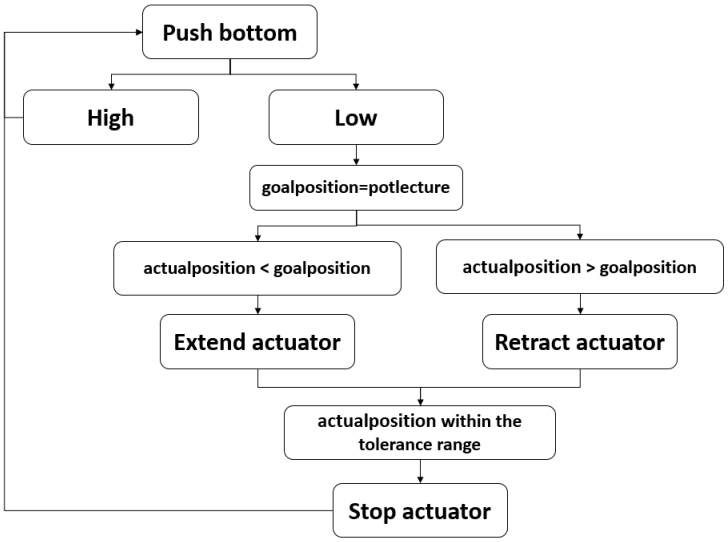

Figure 80 Decision-making block diagram

To perform the action of retracting or extending the actuator, calls have been made to functions defined outside this loop and are explained in the next block. In this way, the code is clearer and more orderly, making it easier to understand, and in there is any error it is easier to locate it.

```
void loop(){
  while (emergencystop == LOW)
  {
    actualposition = analogRead (actuarorPotPin);
    potlecture     = analogRead (potPin);
    Serial.print("   Actuador Pot.=  ");
    Serial.println(actualposition);
    Serial.print("    Pot.=  ");
    Serial.println(potlecture);
     Serial.print("    Goal position.=  ");
    Serial.println(goalposition);

    buttonState = digitalRead(buttonPin);
   if ( buttonState == LOW){
      goalposition = potlecture;
   }
   if (actualposition < goalposition) {
        extendActuator () ;
        if  (actualposition > (goalposition-maxmintolerance) && actualposition < (goalposition+maxmintolerance) ){
            stopActuator ();
        }
   }
   else if (actualposition > goalposition) {
       retractActuator ();
       if  (actualposition > (goalposition-maxmintolerance) && actualposition < (goalposition+maxmintolerance)) {
            stopActuator ();
        }
   }
 }
}
```

Figure 81 Arduino code part 3: main program (Loop)

– **Part 4:** Definition of functions

In this last part of the code, three different functions have been defined (see Figure 82). The first of them corresponds to the function that extends the actuator, which enables relay 2. The second function, which is analogous, executes the retraction of the actuator by enabling relay 1. And the last one, stops the actuator extension or retraction by disabling both relays.

```
void extendActuator ()
{
    digitalWrite(relay1Pin, LOW);
    digitalWrite(relay2Pin, HIGH);
}

void retractActuator ()
{
    digitalWrite(relay2Pin, LOW);
    digitalWrite(relay1Pin, HIGH);
}
void stopActuator ()
{
    digitalWrite(relay1Pin, LOW);
    digitalWrite(relay2Pin, LOW);
}
```

Figure 82 Arduino code part 4: function definitions

5.4. Control implementation and testing

This section will show the assembly of the components described in section 5.2 and the results obtained about how the control system responds.

Firstly, the entire system has been assembled independently from the wind turbine control system, so that it will be much easier to detect any errors and correct them.

In Figure 83, the assembly carried out in the FabLab and the temporary connections made can be seen. Once it is verified that the control system works, each element will be positioned in its corresponding place (see Table 8).

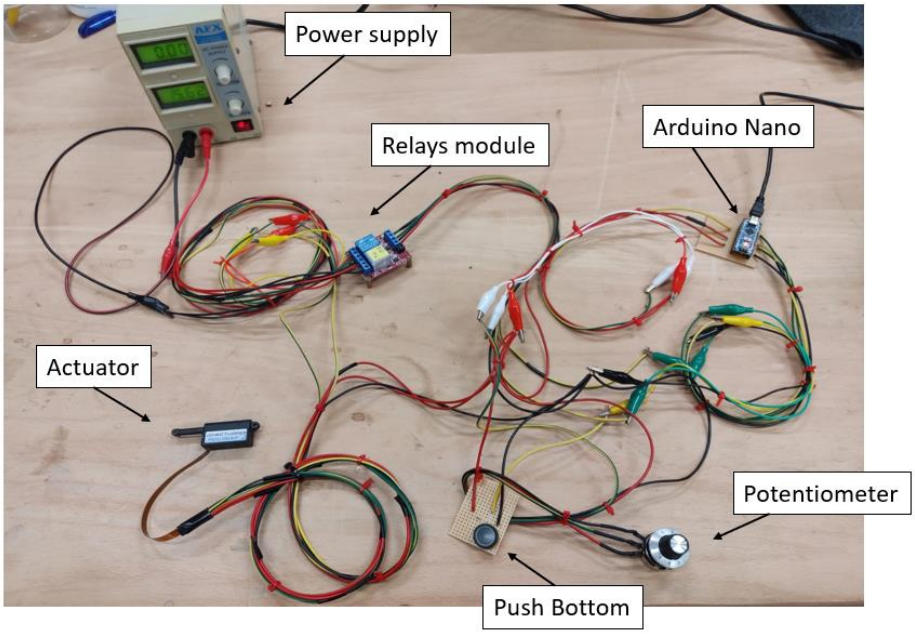

Figure 83 Temporary control circuit connections

Secondly, in order to be able to test the performance of the system, the following points will be checked:

1. External potentiometer measurement
2. Actuator potentiometer measurement
3. Push button operation
4. Reaction of the actuator when the push button is pressed
5. Extreme positions of the actuator (check accuracy).
6. Intermediate positions of the actuator (check accuracy)

To verify those 6 points, 3 different tests will be carried out:

- **Test 1**: checking of potentiometer readings

To check the potentiometer input values (points 1 and 2) it must be ensured that both signals are stable, i.e. do not oscillate in position in the presence of no external action. In addition, when the values of the external potentiometer are varied, the actuator potentiometer must remain constant until the button is pressed.

In Figure 84 it can be seen that indeed the blue signal (corresponding to the actuator potentiometer) remains at the same value over time and is therefore unaffected by variations of the external potentiometer. Furthermore, both signals are stable.

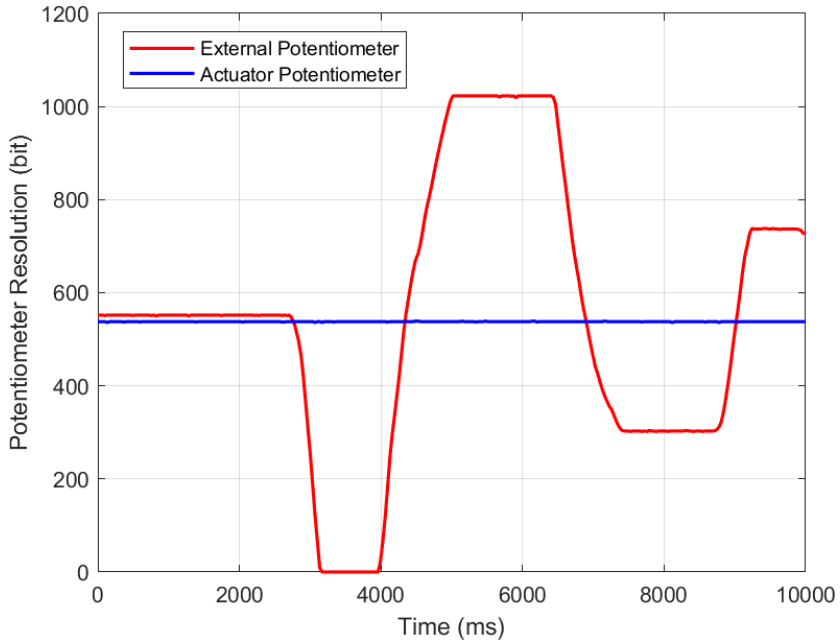

Figure 84 Test 1: Potentiometers lecture

– **Test 2:** button operation and actuator reaction

The following test has shown that when the button is pressed, the actuator starts to move to the position indicated by the external potentiometer. It should be noted that it takes some time for the actuator to reach that position.

The button operation was checked visually, in such a way that the potentiometer was varied to the desired value and at an arbitrary instant the button was pressed. In this way it was verified that, when the button was pressed, the actuator piston did indeed move. The test was repeated 3 times to make sure.

Even though the operation of the button was checked visually, the stored values of the external potentiometer and actuator signals were plotted. From this graph, shown in Figure 85, it is possible to see the reaction of the actuator.

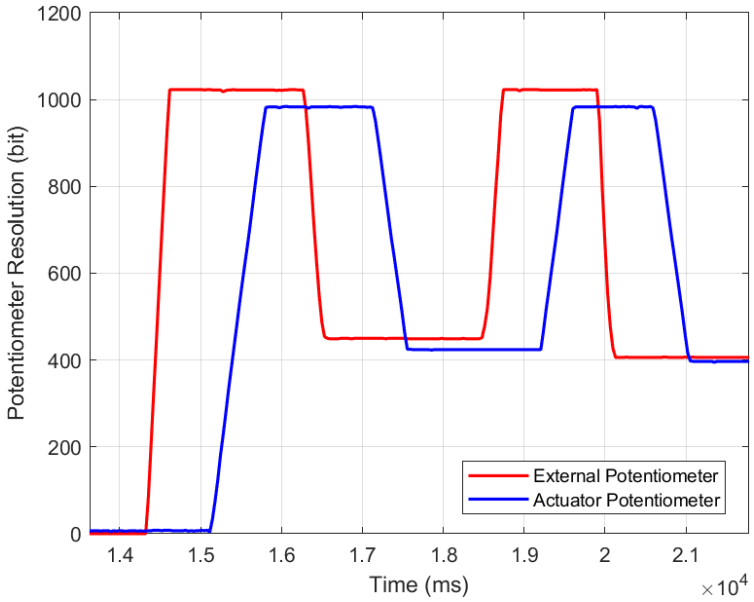

Figure 85 Test 2: button operation and actuator reaction

– **Test 3:** Actuator response accuracy

Finally, the accuracy of the actuator is checked. To avoid oscillations around the desired position, as discussed in the implemented code, a tolerance range has been considered in which if the actuator signal is within this range, the actuator position is considered as valid. This is why in certain positions the signal of the actuator potentiometer (in blue) and the signal of the external potentiometer (in red) do not coincide exactly with each other.

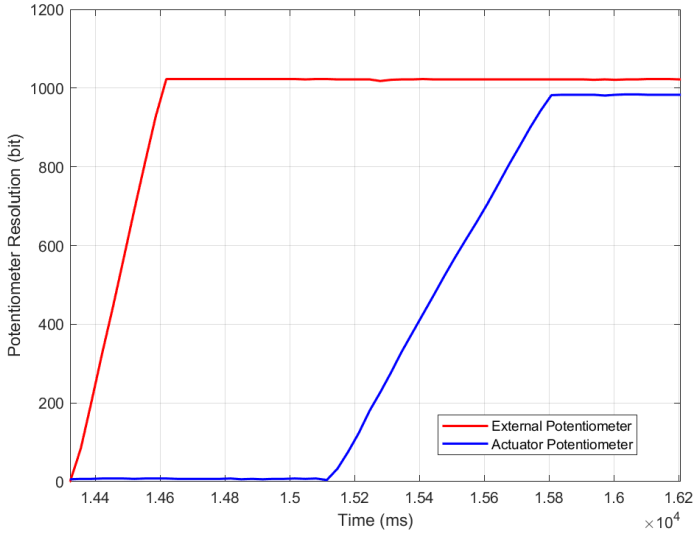

Figure 86 Test 3: Actuator response accuracy

As it can be seen in Figure 86, once the external potentiometer that provides the reference signal is positioned at the desired value, the button is pressed and the actuator moves to that value. Since there is a permanent error due to the tolerance range imposed to avoid oscillations around the desired position, let's see if this error is significant or can be considered despicable.

If we obtain the signal values when both signals have stabilised at the desired position (see Figure 86), the values of the external potentiometer and the actuator are 1021 bits and 983 bits, respectively.

To calculate the relative error between the two values, the following expression is used:

$$relative\ error = \frac{X_{act} - X_{pot}}{X_{pot}} \qquad 31$$

This results in an error of 3.71%, which can be acceptable for this particular application.

Once it has been verified that the control system is working correctly, certain improvements are going to be proposed that will help to make the system more dynamic.

In order to improve the control system, it would be convenient that the tracking of the actuator position to the potentiometer input signal would be automatic, that means, removing the push button. In this way, the desired position would be achieved immediately when the reference potentiometer position is changed. To do this, the code of the main program has been modified, adding the lines shown in Figure 87.

```
postPotLecture = analogRead (potPin);
delay (15);
prePotLecture= analogRead (potPin);
delay(10);
if (postPotLecture != prePotLecture){
   refState = HIGH;
}
if(refState == HIGH){
  goalposition = potlecture;
  refState= LOW;
}
```

Figure 87 Push button replacement code

In this added code, the values of the external potentiometer are compared at two successive time steps and as long as the values remain the same the controller will do nothing. But as soon as these values are different, the rest of the code is executed where the actuator will be extended or retracted as it was before.

The new circuit with the temporary connections can be seen in Figure 88.

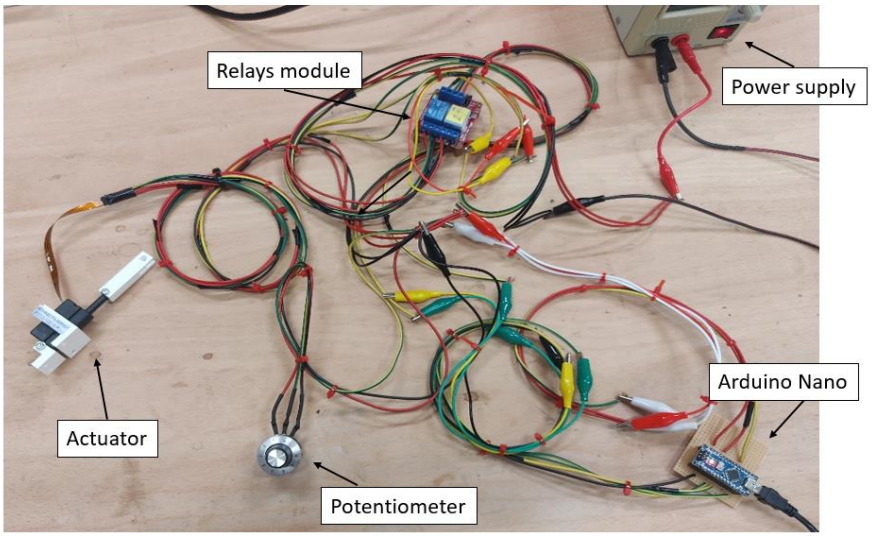

Figure 88 Final control configuration circuit connections without push button

In addition, the new circuit and code have been tested and the data have been exported to a text file so that the results can be analysed using Matlab.

To check the tracking of the actuator against variations of the external potentiometer, the following Figure 89 has been obtained.

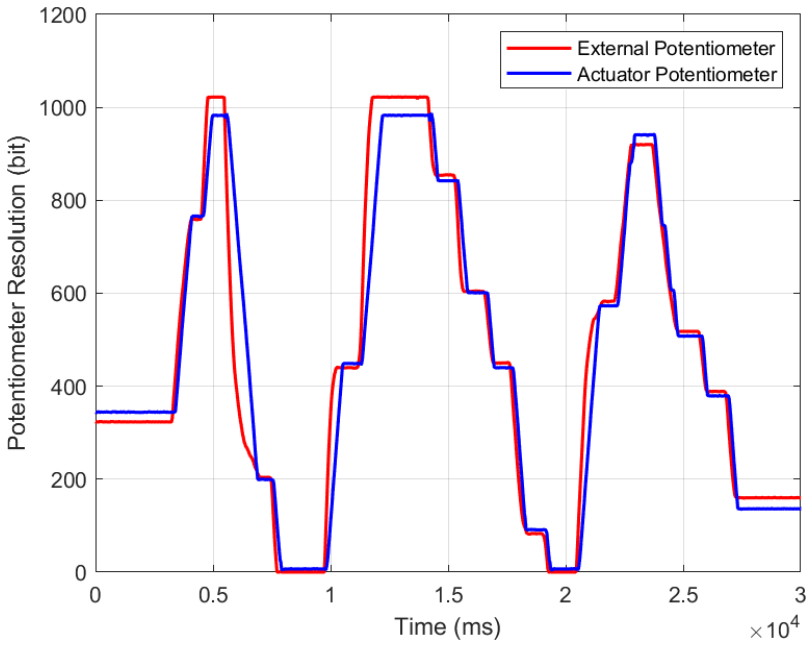

Figure 89 Actuator reaction without push button

In the Figure 89 we can see how the actuator follows the signal from the external potentiometer without problems. If we analyse a shorter time interval we can see in detail the delay that exists from the moment the input values of the potentiometer are varied and the controller sends a signal to the actuator until the actuator makes the movement.

In Figure 90 we can see that in the reduced interval of $858\,ms$ from when the external potentiometer starts to increment until the actuator moves for the first time only $132\,ms$ elapses. And what is more, since the actuator is working at its highest speed, this elapsed time is reduced if we compare the raise time at the desired position. Practically when the potentiometer is placed in the goal position, it takes about $15 \pm 5\ ms$ for the actuator to enter the tolerance range and stabilise.

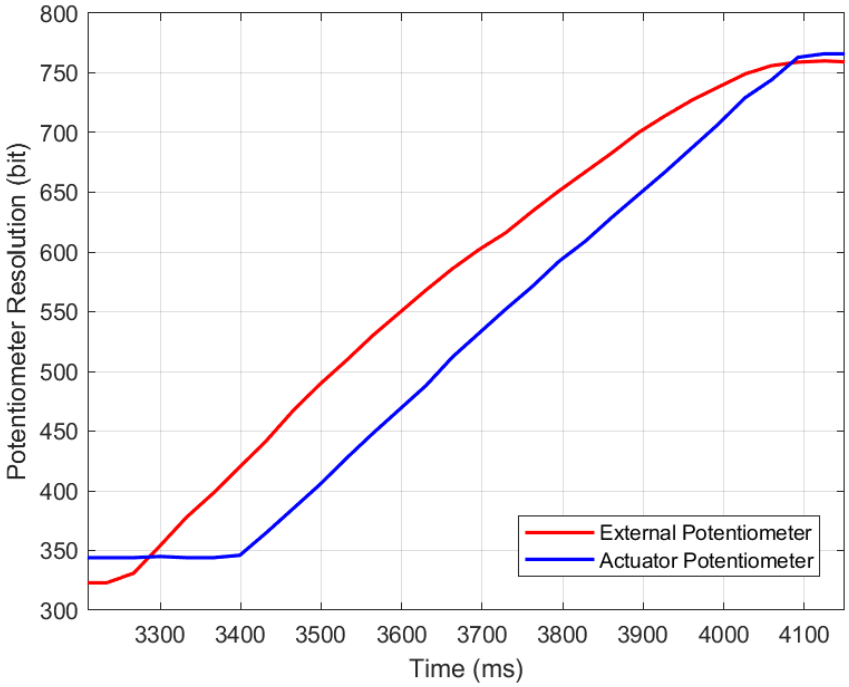

Figure 90 Actuator response in a reduced interval of 1500ms

From the data obtained from the actuator potentiometer, the values of the final pitch angle have been calculated, since we know the relationship between those variables. In addition, Figure 91 shows the comparison between the real values obtained and the theoretical values calculated with the defined equation *17*.

Moreover, from this comparison, the error of each of the points defined in Figure 91 has been calculated and none of them exceeds an error greater than 1.9%, which is acceptable.

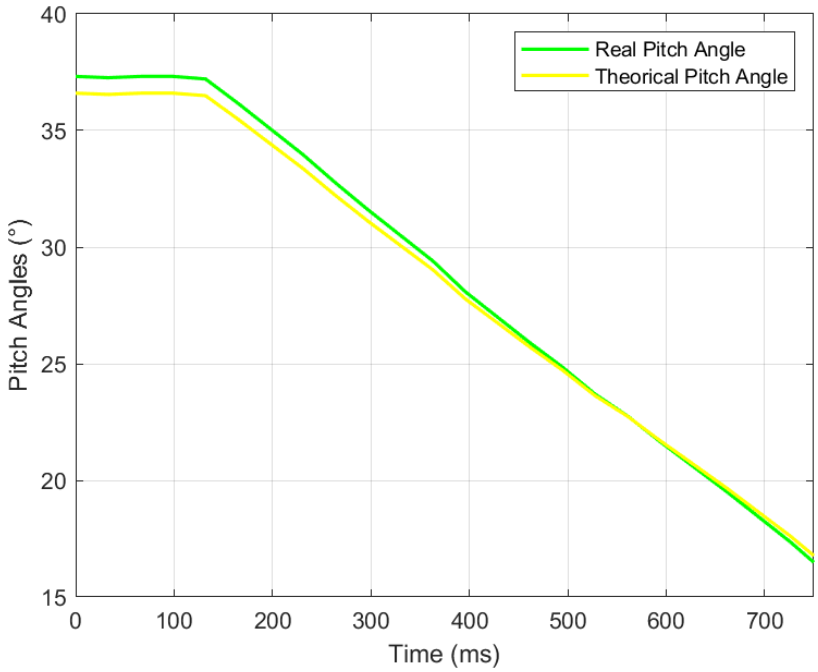

Figure 91 Comparation of the real and theorical pitch angle values

Finally, to be able to compare the reference input signal (external potentiometer) and the final pitch angle define in Figure 91, both signals have been normalise using the following expression:

$$z_i = \frac{X_i - \min(x)}{\max(x) - \min(x)} \qquad 32$$

where,

- $z_i \rightarrow is\ the\ normalised\ value$
- $X_i \rightarrow is\ the\ value\ to\ be\ normalised$
- $\max(x) \rightarrow maximum\ value\ of\ vector\ x$
- $\min(x) \rightarrow minimum\ value\ of\ vector\ x$

Therefore, the following graph has been obtained:

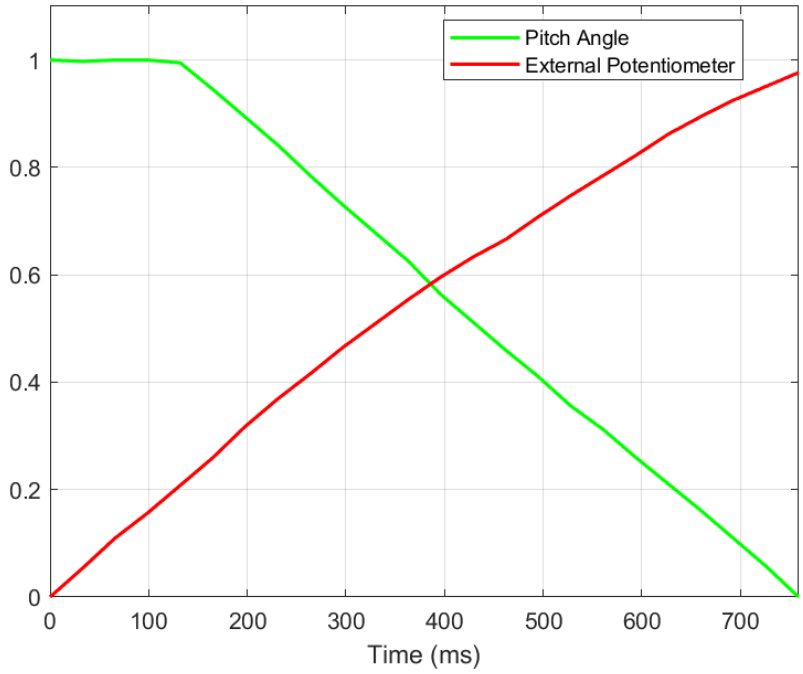

Figure 92 Normalized values of the external potentiometer and pitch angle

From the previous Figure 92, it can be observed the delay that the control system has, and its value corresponds to the horizontal part of the green signal (pitch angle signal) with a value of $132ms$. If we analyse this value, it would correspond to 17.39% of the total time needed to settle at the desired value.

Furthermore, to calculate the response speed of the system and since the reference signal is not a step, but more like a ramp, the actual speed of the control system will be the difference between the speed of the actuator and the speed of the reference signal. In other words, the following expression will be fulfilled:

$$s_{response} = s_{actuator} - s_{ref} \qquad 33$$

In order to obtain the speed parameters, define in equation 33, we only have to calculate the slope of each of the signals. To calculate the slope of the external potentiometer (red signal) and given that it is not exactly a straight line, it will be approximated to a first-degree equation. So, considering this, the final value of the system´s velocity is:

$$s_{response} = 0.031957\,\frac{^\circ}{ms} - 0.026399\,\frac{^\circ}{ms} = 0.005558\,\frac{^\circ}{ms} \qquad 34$$

6. Planning and budget

This section presents the planning of the master thesis and also provides an estimate of the costs involved in the execution of the pitch mechanism and its control.

6.1. Planning

The Work Breakdown Structure (WBS) of the project is shown below, in which the hierarchical organisation and its components can be seen.

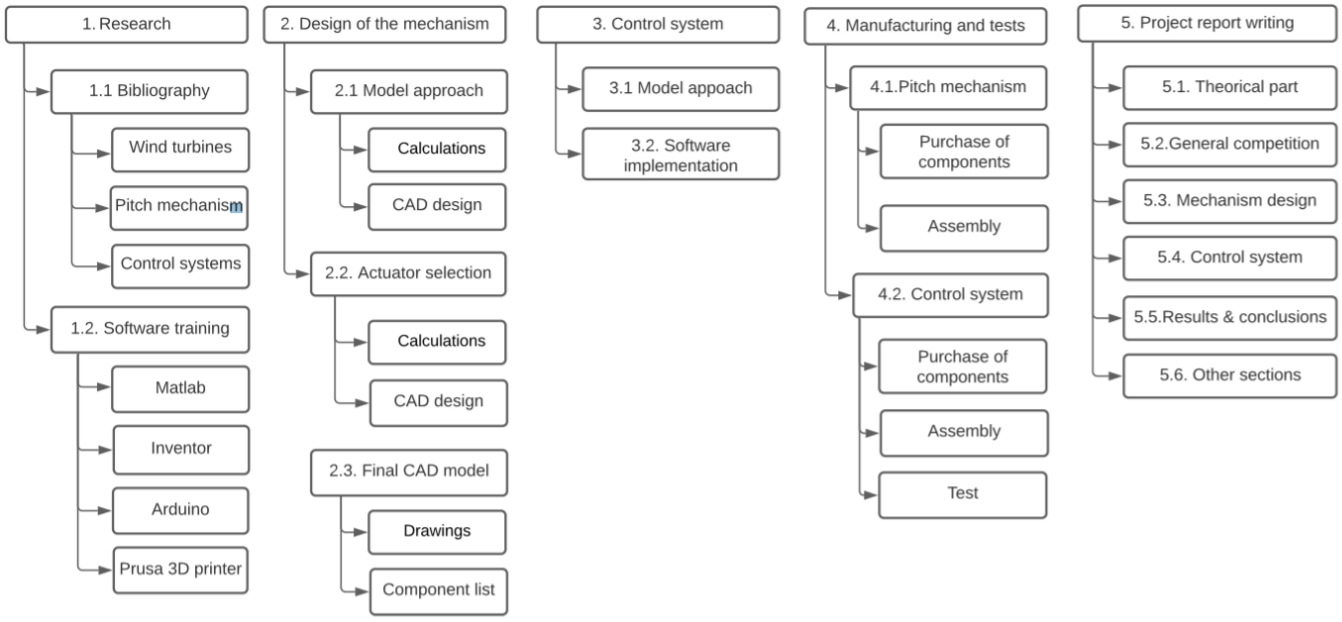

Figure 93 Work Breakdown Structure of the project

And below is detailed, in Figure 94 and Figure 95, the Gantt chart of the project which provides the execution times of the tasks shown in the WBS.

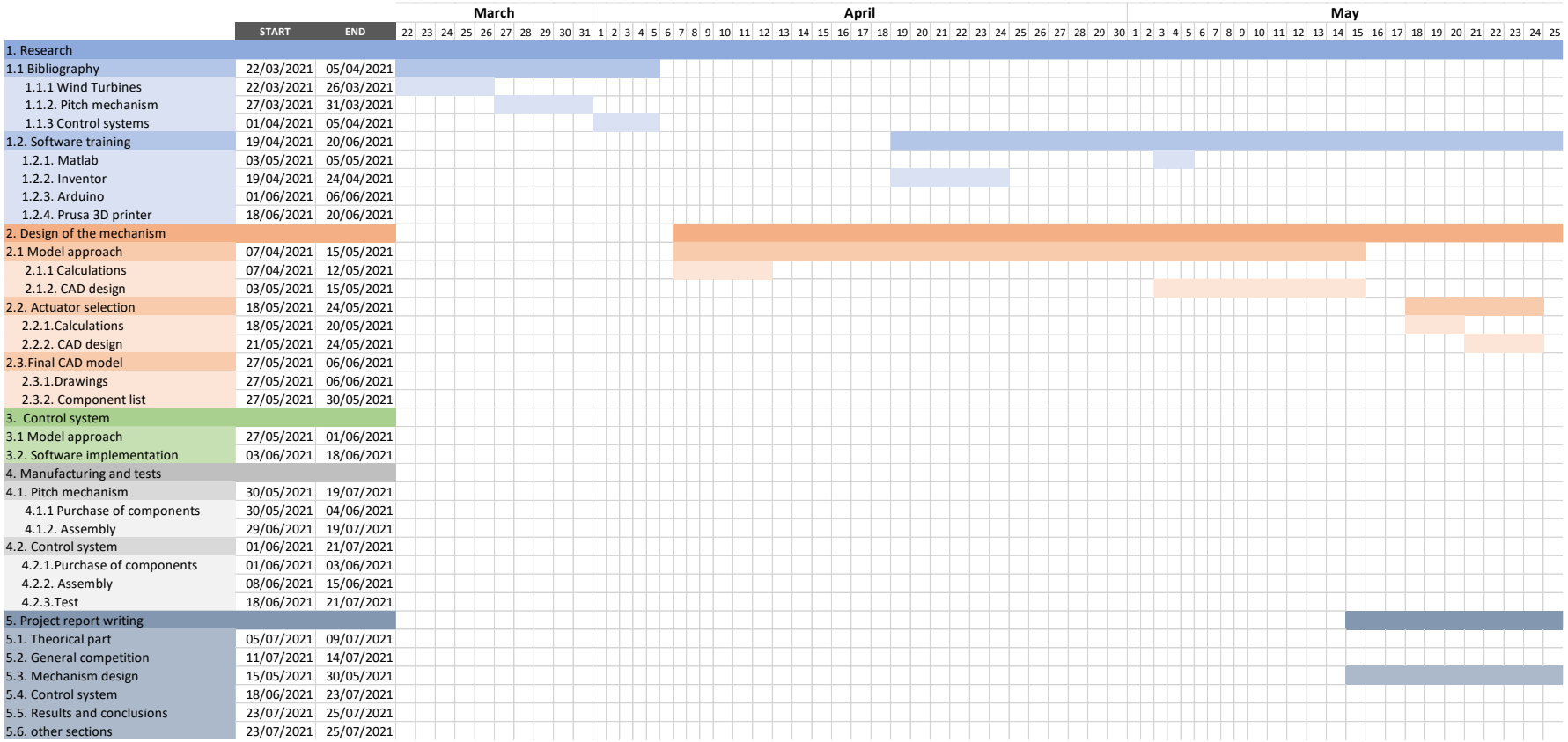

	START	END
1. Research		
1.1 Bibliography	22/03/2021	05/04/2021
1.1.1 Wind Turbines	22/03/2021	26/03/2021
1.1.2. Pitch mechanism	27/03/2021	31/03/2021
1.1.3 Control systems	01/04/2021	05/04/2021
1.2. Software training	19/04/2021	20/06/2021
1.2.1. Matlab	03/05/2021	05/05/2021
1.2.2. Inventor	19/04/2021	24/04/2021
1.2.3. Arduino	01/06/2021	06/06/2021
1.2.4. Prusa 3D printer	18/06/2021	20/06/2021
2. Design of the mechanism		
2.1 Model approach	07/04/2021	15/05/2021
2.1.1 Calculations	07/04/2021	12/05/2021
2.1.2. CAD design	03/05/2021	15/05/2021
2.2. Actuator selection	18/05/2021	24/05/2021
2.2.1.Calculations	18/05/2021	20/05/2021
2.2.2. CAD design	21/05/2021	24/05/2021
2.3.Final CAD model	27/05/2021	06/06/2021
2.3.1.Drawings	27/05/2021	06/06/2021
2.3.2. Component list	27/05/2021	30/05/2021
3. Control system		
3.1 Model approach	27/05/2021	01/06/2021
3.2. Software implementation	03/06/2021	18/06/2021
4. Manufacturing and tests		
4.1. Pitch mechanism	30/05/2021	19/07/2021
4.1.1 Purchase of components	30/05/2021	04/06/2021
4.1.2. Assembly	29/06/2021	19/07/2021
4.2. Control system	01/06/2021	21/07/2021
4.2.1.Purchase of components	01/06/2021	03/06/2021
4.2.2. Assembly	08/06/2021	15/06/2021
4.2.3.Test	18/06/2021	21/07/2021
5. Project report writing		
5.1. Theorical part	05/07/2021	09/07/2021
5.2. General competition	11/07/2021	14/07/2021
5.3. Mechanism design	15/05/2021	30/05/2021
5.4. Control system	18/06/2021	23/07/2021
5.5. Results and conclusions	23/07/2021	25/07/2021
5.6. other sections	23/07/2021	25/07/2021

Figure 94 Project Gantt chart (I)

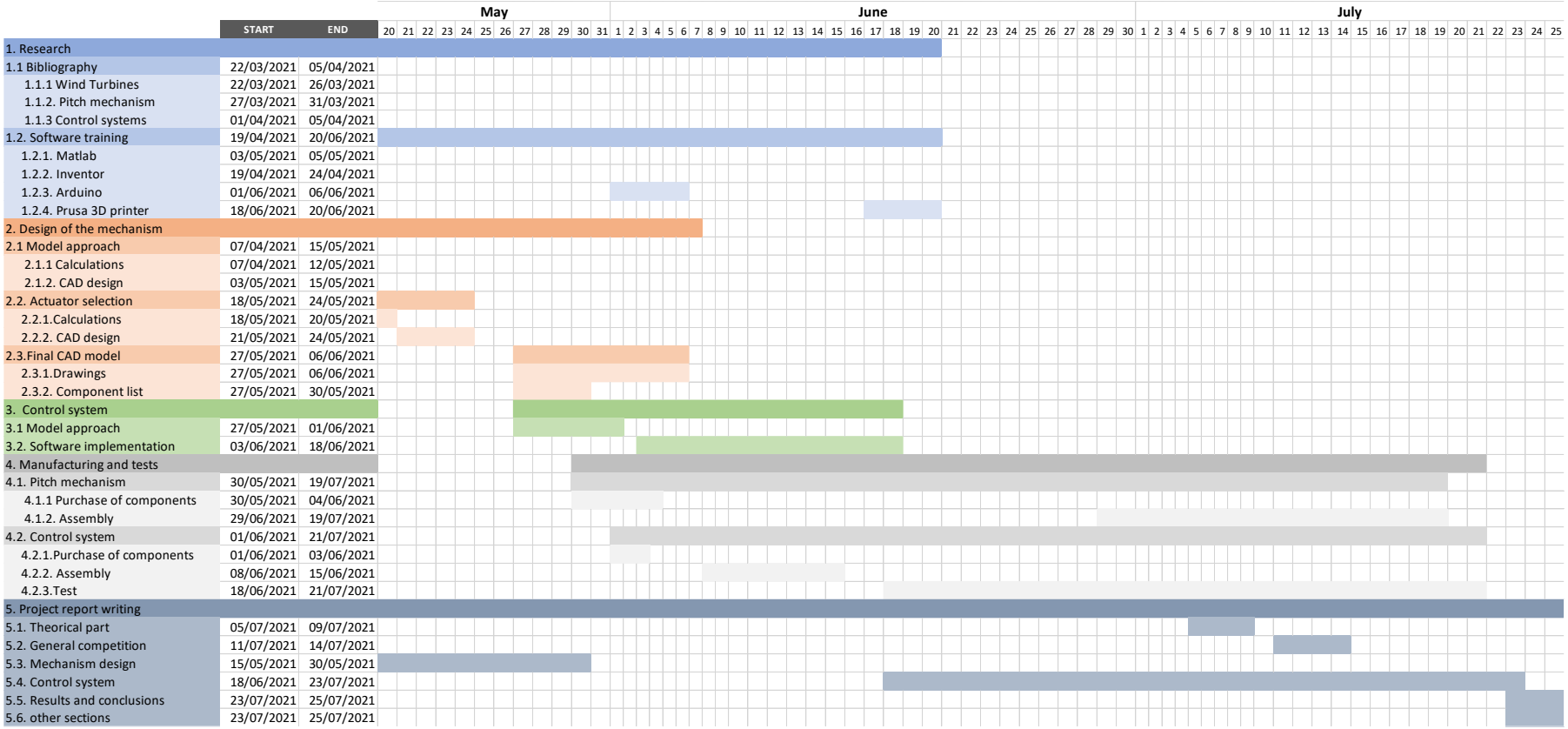

Figure 95 Project Gantt chart (II)

6.2. Budget

For the project budget, the costs will be separated into two categories: the first category shows the costs of the elements necessary to build the pitch mechanism and the second category shows the cost of the elements used to control it.

Table 9 lists all the elements that have been purchased for the assembly of the pitch mechanism prototype.

Table 9 Cost of the components of the mechanical system

Component	Units	Unit price	Total price
Cylindrical plain bearing	1	€ 3.14	€ 3.14
Ball bearing 16009	1	€ 4.65	€ 4.65
Circlips DIN 472	1	€ 3.12	€ 3.12
Circlips DIN 471	1	€ 8.90	€ 8.90
Rod Ball End	6	€ 3.99	€ 23.94
Threaded Rod	1	€ 1.69	€ 1.69
Slide Bushing	3	€ 2.01	€ 6.03
		TOTAL	**€ 51.47**

And in the Table 10 the cost of the elements purchased in order to implement the control of the mechanism have been detailed.

Table 10 Cost of the components of the control system

Component	Units	Unit price	Total price
Arduino Nano	1	€ 7.55	€ 7.55
Jumper Wire Male-Male	1	€ 2.65	€ 2.65
Bread board	1	€ 3.40	€ 3.40
Jumper Wire Female-Male	1	€ 1.00	€ 1.00
Linear actuator	1	€ 116.26	€ 16.26
USB-Mini B	1	€ 2.50	€ 2.50
Relays module	1	€ 2.90	€ 2.90
Push button	1	€ 1.50	€ 1.50
Potentiometer	1	€ 3.50	€ 3.50
		TOTAL	**€ 141.26**

From both tables the total cost of the project can be obtained and this comes to 192.73€ of which 60% of this cost corresponds to the linear actuator.

7. Conclusion

In this last section, some conclusions that have been identified at the end of the project will be presented, as well as some future improvements that can be implemented in the design of the mechanism and the control system.

At this point, we can say that the objectives have been achieved, which were to design a pitch mechanism, manufacture it and control it in such a way that the actuator would be able to position itself with the desired pitch angle.

The design of the pitch mechanism presented is based on a slide-crank mechanism that will slide along the axis of the wind turbine while rotating together with the rotor and hub, which allows the blades of the wind turbine to rotate together on its longitudinal axis.

Prusa's 3D printers have proven to be a fast learning and versatile tool. They have facilitated the manufacture of the first prototype of the pitch mechanism in order to check that the design is capable of executing the movements required by the system. Furthermore, it should be noted that, from a sustainable point of view, the material used for the printing of the prototype (PLA) is a biodegradable polymer, derived from lactic acid and that, being made from renewable resources, it contributes to the environmental sustainability so sought after in these times.

Even so, it would be desirable that in future improvements, both the pitch holding and the pitch disk are manufactured in aluminium in the university workshop. In this way, a more robust and durable mechanism would be obtained.

As for the control system, a system based on on/off control has been implemented, which has archived the objectives we were looking for at this point of the master thesis. In addition, the Arduino platform has proven to be a very useful platform for developing projects of this scale, given that it has a variety of libraries that allow the user to learn its language quickly and easily.

Finally, since the wind turbine was not fully assembled, it was impossible to test the operation of the control together with the rest of the controls and mechanisms. Therefore, as future steps would be to check that there are no operating faults in the control system once the control elements have been mounted on the wind turbine. In addition, it would also be advisable to consider developing a PID control in order to achieve a more precise system, which means that it would be capable of predicting errors and correcting them instantly.

8. References

[1] MAPC, *Clean Energy Toolkit Topic: Wind Energy – MAPC.* [Online]. Available: https://www.mapc.org/resource-library/clean-energy-toolkit-topic-wind-energy/ (accessed: Jul. 16 2021).
[2] J. F. Manwell, *Wind energy explained*. [Place of publication not identified]: Wiley.
[3] *Horizontal Axis Wind Turbine.* [Online]. Available: http://www.top-alternative-energy-sources.com/horizontal-axis-wind-turbine.html (accessed: Jul. 10 2021).
[4] News Powered by Cision, *Siemens Helps Make Vertical Axis Wind Turbine a Reality.* [Online]. Available: https://news.cision.com/siemens-process-industries-and-drives/r/siemens-helps-make-vertical-axis-wind-turbine-a-reality,c9783370 (accessed: Jul. 10 2021).
[5] *Wind Turbines: Upwind or Downwind?* [Online]. Available: http://xn--drmstrre-64ad.dk/wp-content/wind/miller/windpower%20web/en/tour/design/updown.htm (accessed: Jul. 17 2021).
[6] J. Bukała *et al.,* "Small Wind Turbines: Specification, Design, and Economic Evaluation," in *Small Wind Turbines: Specification, Design, and Economic Evaluation*, 2016.
[7] ResearchGate, *(PDF) EVALUATION OF WIND RESOURCES FOR HORIZONTAL AND VERTICAL WIND TURBINE.* [Online]. Available: https://www.researchgate.net/publication/335911538_EVALUATION_OF_WIND_RESOURCES_FOR_HORIZONTAL_AND_VERTICAL_WIND_TURBINE (accessed: Jul. 17 2021).
[8] *Design styles.* [Online]. Available: https://www.wind-energy-the-facts.org/design-styles-7.html (accessed: Jul. 17 2021).
[9] A. Luo, *Journal of Environmental and Account Management, Vol.6, No.3*, 2018.
[10] Rincón Educativo, *Wind Farms.* [Online]. Available: https://www.rinconeducativo.org/es/node/1059 (accessed: Jul. 17 2021).
[11] T. Burton, *Handbook of wind energy*. Chichester: J. Wiley, 2001.
[12] Freude, R. Snurr and D., *Physics of Wind Turbines | Energy Fundamentals.* [Online]. Available: https://home.uni-leipzig.de/energy/energy-fundamentals/15.htm (accessed: Jul. 11 2021).
[13] A. Betz, *Windenergie und ihre Ausnutzung durch Windmühlen,* 1926th ed. Staufen bei Freiburg: Ökobuch, 1994.
[14] Danish Wind Industry Association, *Danish Wind Industry Association*.
[15] B. Zhou, J. Lu, and K. L. Lo, "A Summary Study of Wind Turbine with Related Control," *EPE*, vol. 09, no. 04, pp. 270–280, 2017, doi: 10.4236/epe.2017.94B032.
[16] M. O. L. Hansen, *Aerodynamics of wind turbines*. London: Routledge, 2015.
[17] AviationChief.Com, *Angle of Attack.* [Online]. Available: http://www.aviationchief.com/angle-of-attack.html (accessed: Jul. 11 2021).
[18] E. J. Terrell, W. M. Needelman, and J. P. Kyle, "Wind Turbine Tribology," in *Green Energy and Technology, Green Tribology*, M. Nosonovsky and B. Bhushan, Eds., Berlin, Heidelberg: Springer Berlin Heidelberg, 2012, pp. 483–530.
[19] *Control de potencia en aerogeneradores.* [Online]. Available: http://xn--drmstrre-64ad.dk/wp-content/wind/miller/windpower%20web/es/tour/wtrb/powerreg.htm (accessed: Jul. 11 2021).
[20] H. Geng and G. Yang, "Linear and nonlinear schemes applied to pitch control of wind turbines," *TheScientificWorldJournal*, vol. 2014, p. 406382, 2014, doi: 10.1155/2014/406382.
[21] *International Small Wind Turbine Contest.* [Online]. Available: https://www.hanze.nl/eng/education/engineering/school-of-engineering/organisation/contest/international-small-wind-turbine-contest (accessed: Jul. 12 2021).
[22] *Regulations for the international small wind turbine design contest: ISWTC 2021*, 2021.
[23] R. C. Dorf and R. H. Bishop, *Modern control systems,* 9th ed. Upper Saddle River (New Jersey): Prentice-Hall, 2001.
[24] X-engineer.org, *On-off control system – x-engineer.org.* [Online]. Available: https://x-engineer.org/graduate-engineering/signals-systems/control-systems/on-off-control-system/ (accessed: Jul. 25 2021).
[25] EEEGUIDE.COM, *On Off Controller | Characteristics of Control Action | Effects.* [Online]. Available: https://www.eeeguide.com/on-off-controller/ (accessed: Jul. 13 2021).
[26] *PID controller - Wikipedia.* [Online]. Available: https://en.wikipedia.org/wiki/PID_controller#/media/File:PID_en.svg (accessed: Jul. 13 2021).
[27] *Controlador PID - gaz.wiki.* [Online]. Available: https://gaz.wiki/wiki/es/PID_controller#wiki-3 (accessed: Jul. 13 2021).
[28] *Indian Institute of Technology - Kharagpur* (accessed: Jul. 18 2021).
[29] *Arduino Website.* [Online]. Available: https://www.arduino.cc/

Anexes

A.1. Student team of the University of Applied Science Emden

Florian Saß *Student Ma. Eng. Mechanical Eng.* florian.sass.1@stud.hs-emden-leer.de	***Media Management***
Stefanie Pöttker *Student Ma. Eng. Mechanical Eng.* stefanie.poettker@stud.hs-emden-leer.de	***CAD & FEM*** Blades Hub & Pitch Mechanism
María Roggero Asensio *Student Ma. Eng. Industrial Eng.* maria.rogeero.asensio@stud.hs-emden - leer.de	***CAD & Electronics*** Pitch Mechanism Design and Control
Sascha Hillenbrand *Student Ma. Eng. Mechanical Eng.* sascha.hillenbrand@stud.hs-emden-leer.de	***CAD & Manufacturing*** *Nacelle and breaking system*
Jimmy Gaston Ndagijimana *Student B. Eng. Physical Eng.* jimmy.gaston.ndagijimana@uni-oldenburg.de	***CAD & FEM*** *Tower*
Sönke Schaaf *Student B.Eng. Electrical Eng.* soenke.schaaf@stud.hs-emden-leer.de	***Electronics*** Generator Sensors – Hardware
Fabian Denef *Student B.Eng. Electrical Eng.* fabian.denef@stud.hs-emden-leer.de	***Electronics*** Testing Assembly
Stefan Herten *Student B.Eng. Sustainable Energy Systems* *stefan.herten@stud.hs-emden-leer.de*	***Manufacturing***
Dominik Joswig *Student B.Eng. Sustainable Energy Systems* *dominik.joswig@stud.hs-emden-leer.de*	***Manufacturing***
Marike Pupkes *Student B.Eng. Environmental Eng* *marike.pupkes@stud.hs-emden-leer.de*	***Sustainability***
Sandra Skutella *Student B.Eng. Environmental Eng* *sandra.skutella@stud.hs-emden-leer.de*	***Sustainability***
Chuck Nießit *Student B.Eng. Energy Efficiency* *chuck-lewis.niessit@stud.hs-emden-leer.de*	***Sustainability***

A.2. Supervisors

Prof. Dr.-Ing. Iván Herráez
Professor Wind Energy
ivan.herraez@hs-emden-leer.de

Mohsen Forghani
Scientific assistant
mohsen.forghani@hs-emden-leer.de